Research Article

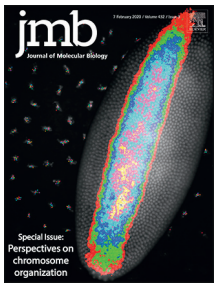

Nucleosome Clutches are Regulated by Chromatin Internal Parameters

Stephanie Portillo-Ledesma [1†], Lucille H. Tsao [1†], Meghna Wagley [1], Melike Lakadamyali [2,3], Maria Pia Cosma [4,5,6,7,8] and Tamar Schlick [1,9,10*]

*1 - **Department of Chemistry,** New York University, 1021 Silver, 100 Washington Square East, New York, NY, 10003, USA*
*2 - **Perelman School of Medicine,** Department of Physiology, University of Pennsylvania, Clinical Research Building, 415 Curie Boulevard, Philadelphia, PA 19104, USA*
*3 - **Perelman School of Medicine,** Department of Cell and Developmental Biology, University of Pennsylvania, Clinical Research Building, 415 Curie Boulevard, Philadelphia, PA 19104, USA*
*4 - **Centre for Genomic Regulation (CRG),** The Barcelona Institute of Science and Technology (BIST), 08003 Barcelona, Spain*
*5 - **Universitat Pompeu Fabra (UPF),** Dr Aiguader 88, 08003 Barcelona, Spain*
*6 - **Institució Catalana de Recerca i Estudis Avançats (ICREA),** Pg. Lluís Companys 23, 08010 Barcelona, Spain*
*7 - **Bioland Laboratory,** Guangzhou Regenerative Medicine and Health Guangdong Laboratory, Guangzhou 510005, China*
*8 - **CAS Key Laboratory of Regenerative Biology,** Guangdong Provincial Key Laboratory of Stem Cell and Regenerative Medicine, Guangzhou Institutes of Biomedicine and Health, Chinese Academy of Sciences, Guangzhou 510530, China*
*9 - **New York University-East China Normal University Center for Computational Chemistry at New York University Shanghai,** Room 340, Geography Building, 3663 North Zhongshan Road, Shanghai, 200062, China*
*10 - **Courant Institute of Mathematical Sciences,** New York University, 251 Mercer St, New York, NY, 10012, USA* [1]

Correspondence to Tamar Schlick: Department of Chemistry, New York University, 1021 Silver, 100 Washington Square East, New York, NY, 10003, USA. *schlick@nyu.edu (T. Schlick)*
https://doi.org/10.1016/j.jmb.2020.11.001
Edited by Anna Panchenko

Abstract

Nucleosomes cluster together when chromatin folds in the cell to form heterogeneous groups termed “clutches”. These structural units add another level of chromatin regulation, for example during cell differentiation. Yet, the mechanisms that regulate their size and compaction remain obscure. Here, using our chromatin mesoscale model, we dissect clutch patterns in fibers with different combinations of nucleosome positions, linker histone density, and acetylation levels to investigate their role in clutch regulation. First, we isolate the effect of each chromatin parameter by studying systems with regular nucleosome spacing; second, we design systems with naturally-occurring linker lengths that fold onto specific clutch patterns; third, we model gene-encoding fibers to understand how these combined factors contribute to gene structure. Our results show how these chromatin parameters act together to produce different-sized nucleosome clutches. The length of nucleosome free regions (NFRs) profoundly affects clutch size, while the length of linker DNA has a moderate effect. In general, higher linker histone densities produce larger clutches by a chromatin compaction mechanism, while higher acetylation levels produce smaller clutches by a chromatin unfolding mechanism. We also show that it is possible to design fibers with naturally-occurring DNA linkers and NFRs that fold onto specific clutch patterns. Finally, in gene-encoding systems, a complex combination of variables dictates a gene-specific clutch pattern. Together, these results shed light into the mechanisms that regulate nucleosome clutches and suggest a new epigenetic mechanism by which chromatin parameters regulate transcriptional activity via the three-dimensional folded state of the genome at a nucleosome level.

© 2020 Elsevier Ltd. All rights reserved.

Please cite tts article as: S. Portillo-Ledesma, L.H. Tsao, M. Wagley, et al., Nucleosome Clutches are Regulated by Chromatin Internal Parameters, *Journal of Molecular Biology*, https://doi.org/10.1016/j.jmb.2020.11.001

Introduction

Chromatin structure, at many levels of spatial and temporal organization, directly impacts gene expression regulation. At the first structural level, approximately 147 base pairs (bp) of DNA[1] wrap around 8 core histone proteins (2 copies of H2A, H2B, H3, and H4) to form the nucleosome,[2] the basic repeating unit in chromatin. The auxiliary protein linker histone (LH) binds to the entry/exit sites of nucleosomes for further compaction.[3,4]. LHs, such as H1,[5] are found in a wide range of densities (ρ), from 0.03 to 1.3 LH per nucleosome,[6] depending on the transcriptional state and type of cell. For example, in vertebrates, the highest LH levels are found in fully differentiated and transcriptional inert avian erythrocytes[7] as well as in heterochromatin of rod photoreceptors in mouse retina.[8] On the other hand, low levels of LH are associated with transcriptionally active cells, such as pluripotent cells.[9] A recent study has shown that besides compacting chromatin directly, LHs also interact with methyltransferases to promote repressive lysine methylation.[10]

Nucleosome positioning is tightly regulated by DNA sequence, transcription factors, and chromatin remodelers that use ATP to facilitate removal, exchange, sliding, or depletion of nucleosomes.[11] Nucleosome placement along the DNA determines the length of the DNA between adjacent nucleosomes (linker DNA). DNA regions depleted of nucleosomes are termed nucleosome free regions (NFRs). NFRs are typically 80–400 bp and are flanked by well-positioned nucleosomes.[12–14] Moreover, nucleosomes do not occupy random positions along the genome; specific patterns have been described for *S. Cerevisiae*,[15] *S. Pombe*,[16] and mouse embryonic stem cells (mESC).[17] Genome-wide nucleosome mapping methods have shown that, in general, (1) promoter regions are depleted of nucleosomes; (2) the first nucleosome downstream of the transcription start site is well localized; (3) nucleosomes at the 5′ end of the gene are more stable than nucleosomes in the middle; and (4) the 3′ end is usually depleted of nucleosomes.[18] Thus, nucleosomes are dynamic and positions alter with cell differentiation,[19] cell cycle stage,[20] metabolic cycle stage,[21] and change in nutrients[22].

Recent *in vivo* and *in situ* data suggest that chromatin fibers are disordered with variable diameters of 5–24 nm,[23,24] in contrast to the dominant 30 nm fiber found *in vitro*.[25] Moreover, emerging evidence from super-resolution microscopy indicates that nucleosomes fold dynamically, and groups of nucleosomes cluster together to establish discrete nanodomains on the kilobase range with different diameters termed "clutches".[26,27] Clutch size (number of nucleosomes) and density (nucleosomes per clutch area) are both heterogeneous within a single nucleus. Such groupings of nucleosomes were identified in cells[28] and also emerge naturally in unfolded trajectories of chromatin fibers, where we identified irregular "superbeads", involving clusters of nucleosomes.[29] Recent micro-C analyses of chromosome folding *in vivo* have shown that tri or tetra-nucleosomal folding motifs are present in yeast[30] and that small groups of ~3–10 nucleosomes recur in mammalian cells.[31] Here, we define nucleosome clutches as spatial groups of at least three nucleosomes no more than 20 nm apart and distinct from other groups of nucleosomes by more than 20 nm. Our clustering algorithm (see Methods) measures these precisely as a function of input parameters.

These nucleosome clutches appear to be regulated by the differentiation state of the cell, as their size and density correlates with the cell pluripotent grade. For instance, somatic cells, with compact chromatin containing higher levels of LH, appear to have larger and denser nucleosome clutches than pluripotent cells,[26] which have an "open" chromatin structure and lower levels of LH.[9,32] In another super-resolution microscopy study, we further showed that histone tail acetylation, a common post translational modification found in active chromatin regions,[33] affects DNA compaction within nucleosomes.[34] A lower amount of DNA was found to be associated with nucleosome clutches in hyperacetylated cells, linking the epigenetic state of the clutch to the DNA packing inside the clutch.[34] These findings are in agreement with modeling studies that have shown an overall chromatin decompaction upon acetylation due to the impairment of nucleosome/nucleosome interactions that stabilize chromatin's tertiary structure.[35,36]

When chromatin is highly compact, it becomes inaccessible to cellular enzymes that control various genomic functions, such as DNA transcription, replication, and repair.[37] However, when chromatin is decompacted, the DNA is readily available for transcript-reading processes.[37] Since chromatin structure plays such a key role in gene expression, new mechanistic insights into gene regulation during cell differentiation are valuable.

To gain insight into the mechanisms regulating nucleosome clutches, we perform a systematic study to explore the effects of chromatin internal parameters on clutch patterns. We use our nucleosome resolution chromatin mesoscale model[38,39] with variable nucleosome positions, linker histone density, or histone tail acetylation (Ac) levels in the context of general fibers and specific genes. We analyze clutch patterns in uniform chromatin fibers of 100 nucleosomes (~20 kbp), non-uniform fibers of 50 nucleosomes (~10 kbp) with naturally-occurring DNA linker lengths, and two gene-encoding fibers, HOXC (~50 kbp) and Pou5f1 (~30 kbp).

Our results reveal that the main factor regulating clutches in uniform fibers is nucleosome placement, in particular, the length of nucleosome free regions. Linker histone density is the next controlling variable; higher densities produce larger clutches by a chromatin compaction mechanism. Finally, the Ac levels appear to modulate the nucleosome clutches by a configuration-dependent chromatin unfolding mechanism. With this knowledge, we design *in silico* non-uniform chromatin fibers that fold onto target clutch patterns, such as few large and small clutches induced by low LH density, several NFRs, and Ac islands; a "pearl necklace" structure, encouraged by small and equally spaced groups of nucleosomes, high LH density, and several NFRs; and varied-size clutches, induced by groups of nucleosomes of different size, several NFRs of different size, and no LH nor Ac. Finally, our results on the gene-encoding fibers indicate that the specific combinations of all these parameters dictates a folding pattern on both global and local levels that cannot easily be deduced from the sum of the parts.

Overall, our results highlight the mechanisms involved in the regulation of clutch patterns and suggest how such regulation could affect gene expression. Through the regulation of nucleosome positions, LH density, and Ac levels, gene expression can be controlled by the formation of large/compact or small/loose clutches that hinder or facilitate accessibility to the cellular transcriptional machinery.

Methodology

Systems setup

Effect of nucleosome positions, LH density, and Ac levels on uniform fibers. To determine the effect of nucleosome positions on clutch formation, we generate starting configurations for chromatin fibers of 100 nucleosomes with initial coordinates corresponding to an ideal zigzag conformation oriented with the fiber axis parallel to the z-axis, as we have shown this conformation to have the lowest energy.[40]

We consider the following systems:

(a) Uniform fibers without NFRs. We select short, medium, and long DNA linker lengths (LLs) of 26, 44, and 79 bp, respectively, based on the DNA linker lengths distribution in mouse embryonic stem cells (mESC) determined by Voong et al.[17] and the DNA linker lengths that our model can represent due to the ~9 bp resolution.[17,41].
All fibers are simulated with a linker histone (LH) density of 0.5 LH per nucleosome, as previously determined for mESC,[9] with LHs distributed uniformly. No histone tail acetylation (Ac) is considered. See Figure S1 of SI for starting configurations.

(b) Uniform fibers with NFRs. Each short, medium, and long uniform fiber is modeled with short, medium, and long NFRs. Based on the typical length of NFRs, between 80 and 400 bp,[12–14] we consider NFRs of 114, 220, and 326 bp, and distribute them uniformly as 1 NFR every 10 nucleosomes.
The LH density is also set to 0.5 LH per nucleosome,[9] with LHs distributed uniformly. No Ac is considered. See Figure S2 of SI for starting configurations.

(c) LH density variability. We consider two of the systems from (b). (1) The uniform fiber with long LLs (79 bp) and medium NFRs (220 bp) placed every 10 nucleosomes without LH and with 0.25, 0.5, 0.75, and 1 LH per nucleosome. (2) The uniform fiber with short LLs (26 bp) and short NFRs (114 bp) placed every 10 nucleosomes without LH and with 0.5 and 1 LH per nucleosome.
In both systems LHs are distributed uniformly along the chromatin fiber to satisfy the different densities. No acetylation is considered. See Figure S3 of SI for starting configurations.

(d) Ac levels. We consider two of the systems from (b). (1) The fiber with short DNA linker lengths (26 bp) and short NFRs (114 bp) placed every 20 nucleosomes, without acetylation and with 25, 50, 75, and 100% of tails acetylated. We reduce the number of NFRs from 10 to 5 to decrease flexibility. We further study the same system with 10 NFRs without acetylation and with 50 and 100% of tails acetylated. (2) The fiber with long LLs (79 bp) and 10 medium NFRs (220 bp) without acetylation and with 50 and 100% of tails acetylated.

In all the systems we distribute the acetylations in two islands at the beginning and at the end of the fiber, mimicking trends *in vivo*.[42] No LH is considered. See Figure S4 of SI for starting configurations.

The above studies are performed as the monovalent salt concentration of 150 mM, typical for physiological conditions. We also perform a set of simulations with our first-order approximation for divalent ion conditions.[43] Here we consider such fiber systems in combination with: (1) DNA linker length = 26 bp and 10 NFRs = 114, 220, or 326 bp; (2) DNA linker length = 79 bp and 10 NFR of 220 bp with different LH densities (0–1 LH/nucleosome); and (3) DNA linker lenght = 26 bp and 5 NFRs = 114 bp with different Ac levels (0–100%).

Design of fibers with naturally-occurring DNA linker lengths. We design 50-nucleosome non-uniform fibers with naturally-occurring DNA linker lengths and NFRs that fold onto specific clutch patterns. We mimic the DNA linker length distribution determined by Voong et al. as approximately 30% of linker DNA with 26 bp; 18% with 35 bp; 14% with 44 bp; 12% with 53 bp; 8% with 62 bp; 8% with 71 bp; and 10% with 79 bp.

The linker DNAs are distributed randomly.[17] We distribute short (114 and 167 bp), medium (220 bp), and long (326 bp) NFRs, LHs, and Ac, as described below.

The designs have the following parameters:

(a) Design 1: One large clutch and one small clutch. We apply a LH density of 0.7 LH per nucleosome and position LHs at nucleosomes 1 – 20, 31 – 36, and 42 – 50. We prescribe 9 NFRs to separate these three groups of nucleosomes: 5 short NFRs of 114 bp between nucleosomes 22 and 23, 24 and 25, 26 and 27, 30 and 31, and 39 and 40; and 4 NFRs of 167 bp between nucleosomes 21 and 22, 28 and 29, 37 and 38, and 41 and 42. The irregular by values NFRs come from the ~ 9 bp resolution in our linker DNA model.[44] We further acetylate nucleosomes between the three groups of nucleosomes, namely 21–30 and 37–41.
(b) Design 2: Pearl necklace-like structure. We use a LH density of 1 LH per nucleosome and no acetylation. We include 12 medium NFRs, positioned every 4 nucleosomes.
(c) Design 3: Variable-sized clutches. We use 5 NFRs to separate groups of nucleosomes of different size. Specifically, we prescribe 2 short NFRs of 167 bp between nucleosomes 3 and 4, and between nucleosomes 45 and 46. Additionally, we place 3 long NFRs between nucleosomes 11 and 12, 20 and 21, and 31 and 32. No LH nor acetylation is considered.

Effect of LH density and Ac levels on HOXC and Pou5f1 genes. To determine how LH density and Ac levels regulate nucleosome clutches in gene systems, we study gene-encoding systems with different LH densities and histone tail acetylation levels. Specifically, we study the human HOXC gene locus which encodes proteins involved in embryonic development[45] and the mouse Pou5f1 gene loci that codes for oct4, a transcription factor involved in cell differentiation. Both systems have been previously studied by our group.[46,47]

The HOXC system was simulated with the same parameters as before,[47] except for changing LH density or Ac levels when studying their effect on clutch formation. DNA linker lengths are modeled using the distribution from chemical mapping in mESC determined by Voong *et al.*[17]; NFRs are determined using micrococcal nuclease sequencing (MNase-seq) data[48]; LHs are located to simulate trends in mESC[49]; and tail acetylations are located based on Chip-Seq data (Table S1).

Similar to uniform fibers, to determine the effect of tail acetylation, we model the systems without acetylation and with increasing levels of acetylation so as to reach 50% and 100% of tails acetylated; the acetylated nucleosomes are distributed in two islands located at the beginning and end of the gene.

To determine the effect of LH density in the context of acetylation, we simulate fibers without LH and with of 0.5 and 1 LH per nucleosome, distributed uniformly. See Figure S5 of SI for starting configurations. We further analyze the trajectories of the native HOXC[47] to compared it with the systems studied in this article.

The Pou5f1 system represents chromatin in somatic cells. We simulate it as before,[46] except for changing LH density or Ac levels when studying their effect on clutch formation. Nucleosome positions are modeled based on publicly available MNase-seq data,[50] LH density is set to 0.8 LH per nucleosome with LHs uniformly distributed,[32] and Ac levels are set to 10% with acetylated nucleosomes distributed in two islands to mimic realistic distributions[42] (Table S1). Similar to HOXC, we study three LH densities, 0, 0.5, and 1 LH per nucleosome, and three Ac levels, 0, 50, and 100%. We also report the average number of nucleosomes per clutch for the native Pou5f1 determined previously.[46] See Figure S6 of SI for starting configurations.

Chromatin mesoscale model

Our chromatin mesoscale model has been developed along with emerging experimental data for over two decades and validated for various structural and dynamical measurements.[41,51–53] For example, early fiber structure models reproduced sedimentation coefficients and salt-dependent condensation of fibers.[40,51,54] By incorporating linker histone, we reproduced fibers obtained with Cryo-EM,[55] and by incorporating magnesium effect implicitly, we reproduced the magnesium-dependent compaction of chromatin observed with EMANIC.[43] With a dynamic LH binding model, along with a force-pulling code, we reproduced experimental force-pulling profiles.[56] Regarding nucleosome clutches, we recently studied chromatin organization at the nucleosome level by combining mesoscale modeling of chromatin fibers with single molecule tracking of nucleosomes.[46] By simulating chromatin fibers typical of mouse embryonic stem cells and neural progenitors, we showed agreement between nucleosome clutches at a single locus level with clutches observed by super-resolution microscopy[26] and micro-C[31] studies at a genome-wide level.

The fibers are simulated using our nucleosome-resolution coarse-grained mesoscale model that describes chromatin components at different levels of resolution.[38] The nucleosome core with 147 bp of DNA wrapped around and without histone tails is coarse-grained from the atomistic nucleosome[57] as an electrostatic rigid body. It contains 300 Debye-Hückel charges computed by our DiSCO algorithm[58,59] that correctly and economically describe the electrostatic field of the atomistic

nucleosome predicted by the Poisson–Boltzmann formulation. Flexible histone core tails are coarse-grained as 5 amino acids per bead with the Levitt-Warshel united-atom bead model.[55] Acetylated tails are modeled as folded and rigid tails following our all-atom and multiscale study of histone acetylation.[35] There, by modeling acetylated tails with several force fields and all-atom Replica Exchange molecular dynamics, we found that acetylation increases the tails secondary-structure order, producing rigid and folded tails. These folded tails were coarse-grained and introduced into our mesoscale model. In practice, this was implemented by increasing the force constants (by a factor of 100) for the stretching, bending, and torsional potentials so that the tails maintain their folded structure. Monte Carlo simulations of chromatin fibers with these "folded" tails, as well as with flexible tails but with a charge reduction of 1e, revealed that acetylation marks do not induce fiber decompaction through a charge neutralization mechanism per se, but through a multiscale mechanism that involves the loss of stabilizing internucleosome interactions due to a more rigid and folded tails upon acetylation. Linker DNA is treated with a combined worm-like chain and bead model.[44] Each bead has a negative salt-concentration dependent charge derived by Stigter's procedure,[60] and the model has a resolution of ~9 bp and inter-bead segment of 3 nm. The LH H1E is derived from the all-atom structure of the rat H1.4, and coarse-grained as histone tails: 6 beads for the globular head and 22 beads for the C-terminal domain.[53] We neglect the N-terminal domain since it has a minor role in organizing higher-order chromatin structure.[61] Finally, the presence of Mg^{2+} is modeled by the phenological approach we developed in Ref. 43, where we reduce the electrostatic repulsion among linker DNAs by increasing the Debye length from 1.52 nm^{-1} to 2.5 nm^{-1} in the Debye-Hückel term corresponding to the DNA-DNA interaction. This allows linker DNA beads to approach each other closely. We also reduce the DNA persistence length from 50 to 30 nm based on experimental data.[62]

The total energy function of the model includes stretching, bending, and twisting modified worm-like chain terms to describe the DNA beads; stretching and bending terms to describe histone tails and linker histones; Debye-Hückel terms for all elements of the system to describe electrostatics; and Lennard-Jones potential terms to avoid steric clashes for all elements in the system. Model details and parameters can be found in Refs. 38,55.

Conformational sampling and ensemble generation

To obtain an ensemble of configurations in thermal equilibrium, we perform Monte Carlo (MC)[39] sampling of fibers from zigzag starting configurations, dominant under the conditions used here (intermediate monovalent salt concentration and presence of linker histone).[43] To approximate physiological conditions, simulations are performed at a salt concentration (NaCl) of 150 mM and a temperature of 293 K.

We use four tailored sampling movements: (1) a local translation move in which an element (core/DNA bead) is selected and translated about a randomly chosen axis by a random distance (<0.6 nm); (2) a local rotation move in which a selected element is rotated around one of its axes; (3) a global pivot move in which an element is selected and then the shorter end of the oligonucleosome is rotated randomly about a randomly selected axis passing through that element; and (4) a regrowth move for the tails that uses a configurational bias Monte Carlo approach in which a histone tail is selected and fully regrown in a bead-by-bead fashion. Local translation, rotation, and global pivot movements are accepted or rejected according to the regular Metropolis criteria,[63] whereas acceptance of a regrow move is based on the Rosenbluth criteria.[64]

All systems are run for 50–80 million MC steps and the last 10 million steps are used for analysis, following convergence checks for local and global geometric and energetic variables. Each trajectory starts from a different initial pseudo random number generator and a different DNA twist value of −12°, 0°, or +12° to mimic natural variations in the B-DNA twist.[65] Results are averaged over ensembles of 20 trajectories containing 2000 configurations.

Structural analysis

Clustering analysis. Nucleosome clusters are quantified using the Density-based clustering algorithm (DBSCAN),[66] as implemented in MATLAB. DBSCAN discovers clusters in noisy data by partitioning the n-by-n internucleosome distance matrix into clusters. This partition is based on two parameters, the minimal number of data points to define a cluster (*minpts*) and the distance that specifies if two points belong to the same cluster (*epsilon*). Here, we use a *minpts* of 3 nucleosomes and an *epsilon* of 20 nm. Thus, nucleosome clutches are defined as groups of at least 3 nucleosomes no more than 20 nm apart. Importantly, the clustering algorithm is applied to folded fibers, as we are interested in the spatial clutches established upon folding.

The algorithm identifies three kinds of points: core, border, and noise points based on a threshold for *epsilon* and the *minpts*. Any point *x* in the dataset with a neighbor count greater than or equal to *minpts* is selected as a *core point*. On the other hand, if the number of neighbors is less than *minpts*, but the point *x* belongs to an *epsilon* neighborhood of some *core point z*, the point is

identified as a border point. Finally, if a point is neither a core nor a border point, which means it is not reachable through any point from a core point, it is identified as a *noise point* and is not part of any cluster.

The algorithm is implemented as follows:

1. From the input data set, select the observation *x1* and assign it to cluster 1
2. Find the set of points within the *epsilon* neighborhood of the current point
   a. If the number of neighbors is less than *minpts,* label the current point as noise. Go to step 4.
   b. If not, label the current point as a core point belonging to cluster 1.
3. Iterate over each neighbor (new current point) and repeat step 2 until no new neighbors that can be labeled as belonging to the current cluster are found.
4. Select the next observation, *x2,* as the current point and increase the cluster count by 1.
5. Repeat steps 2–4 until all points in the input data set are labeled.

If the distance between two border points belonging to different clusters is smaller than *epsilon*, DBSCAN merges the two clusters into one.

The *minpts* and *epsilon* parameters were chosen based on the heuristic provided by the algorithm developers.[67] *Minpts* was selected as 3 nucleosomes as it is recommended to be at least $\geq D+1$, where D is the number of dimensions in the data set. However, this parameter does not significantly affect the overall results of the clustering.[67] The radius, *epsilon*, was selected as 20 nm based on the fiber dimensions.

For each ensemble, we calculate the average number of nucleosomes per cluster and the number of clusters. We also determine the average compaction of the nucleosomes inside the clusters as the ratio of number of nucleosomes to area for each cluster. The area is determined with the *AlphaShape* function native to MATLAB which creates a bounding area that represents a polygon that envelops the nucleosomes of each clutch.

Compaction and fiber morphology parameters.

(1) The sedimentation coefficient ($S_{w,20}$), in units of Svedbergs, is used to describe the compaction of the fiber. It is measured by the relation:

$$S_{w,20} = ((S_1 - S_0) * LH_{conc} + S_0) * \left(1 + \left(\frac{R_1}{N_C}\right) \sum_i \sum_j \frac{1}{R_{ij}}\right), \quad (1)$$

where S_0 is the sedimentation coefficient for a mononucleosome with LH bound (12 S),[68] S_1 the sedimentation coefficient for a mononucleosome without LH (11.1 S),[69] LH_{conc} the concentration of LH in the fiber, R_1 the spherical radius of a nucleosome (5.5 nm), N_C the number of nucleosomes in the fiber, and R_{ij} the distance between two nucleosomes *i* and *j*.

(2) The radius of gyration, which describes the overall dimension of the polymer chain, is measured as the root mean squared distance of each nucleosome from the center of mass according to the relation:

$$R_g^2 = \frac{1}{Nc} \sum_{j=1}^{N} (r_j - r_{mean})^2 \quad (2)$$

where *Nc* is the number of nucleosomes, r_j the center position of the nucleosome core *j*, and r_{mean} the average of all core positions.[41]

(3) Fiber volumes are calculated using the *AlphaShape* function native to MATLAB that creates a bounding volume that envelops all the nucleosomes of the fiber.

(4) Fiber widths are calculated as twice the average between the nucleosome center and the fiber axis. From the fiber axis, we define the local fiber radius for a given nucleosome as the perpendicular distance between a nucleosome core center and its closest linear fiber axis segment plus the nucleosome radius (5.5 nm). All local fiber radii in a given fiber are averaged to obtain the fiber radius.

The fiber axis is defined as a 3D parametric curve $r^{ax}(s) = (r_1^{ax}(s), r_2^{ax}(s), r_3^{ax}(s))$ where each component $(r_j^{ax}(s), j = 1, 2, 3,)$ refers to the *x*, *y*, *z*, are parametric curve components. The fiber axis is then fitted into a polynomial form:

$$r_j^{ax}(s) \approx P_j(i) = p_1{}^n(s) + p_2{}^{n+1}(s) + \cdots + p^n(s), \quad (3)$$

where the polynomial degree is chosen using the MATLAB *polyfit* function so that the fiber axis fits a standard least-squares fitting procedure.

Nucleosome/nucleosome interactions. Contact probability matrices describe the fraction of MC steps in which the tail or core of nucleosome *i* are within 2 nm of the tail or core of nucleosome *j*. Contacts are written in a base pair or nucleosome resolution matrix every 1 million MC steps. Contact probabilities are normalized across all frames of the trajectory.

Histone tail interactions. Interactions between tails and other chromatin elements are calculated as the fraction of MC steps in which the tail beads are within 2 nm of parental DNA, parental core, non-parental DNA, non-parental core, or tails of a different nucleosome. Distances are measured from the center of the end tail bead, from the geometric center of the entire nucleosome core, and from the center of each linker bead. The interactions are sampled across the ensembles of 2000 configurations and normalized across all the sampled structures. Tail interactions are averaged over both copies of each tails.

Results

Uniform fibers without NFRs do not form nucleosome clutches and their global folding is affected by the length of linker DNA

To determine the effect of nucleosome positions on the regulation of clutch patterns, we simulate uniform fibers with short (26 bp), medium (44 bp), and long (79 bp) DNA linker lengths and without NFRs.

Representative chromatin fiber structures (Figure 1(a)) do not show discrete nucleosome clutches, even for the fiber with the longest linker DNA. This occurs because in fibers without NFRs all nucleosomes are in close proximity upon folding, creating a single group of nucleosomes. To establish a clutch, a group of nucleosomes has to be separated by more than 20 nm from another nucleosome or group of nucleosomes. Thus, NFRs separate nucleosomes into discrete groups or clutches, in agreement with experimental observations.[26] However, the global folding of the fiber is affected dramatically by the length of linker DNA. Internucleosome contact maps (Figure 1(a)) show the presence of only short-range interactions in the system with short and medium DNA linker lengths, with mostly $i \pm 1$ and $i \pm 2$ interactions, typical of a ladder-like conformation which arise from the repulsion due to the short linkers. The fiber with long DNA linkers exhibits presence of medium and long-range interactions, with $i \pm 1$, 2, 3, 4, 5, 6, and >7 interactions, indicative of higher-order folding motifs such as hairpins and hierarchical looping, or stacked loops.[70]

Corresponding fiber widths are 40 ± 2 nm for long-linker, 32 ± 4 nm for medium-linker, and 31 ± 1 nm for short-linker DNA. This difference results from the interdigitation of nucleosomes from successive helical gyres in fibers with long-linker DNA, resulting in a more compact fiber, in agreement with experiments.[71]

The radius of gyration (Figure 1(b)) decreases from 70 ± 16 nm in short-linker fibers to

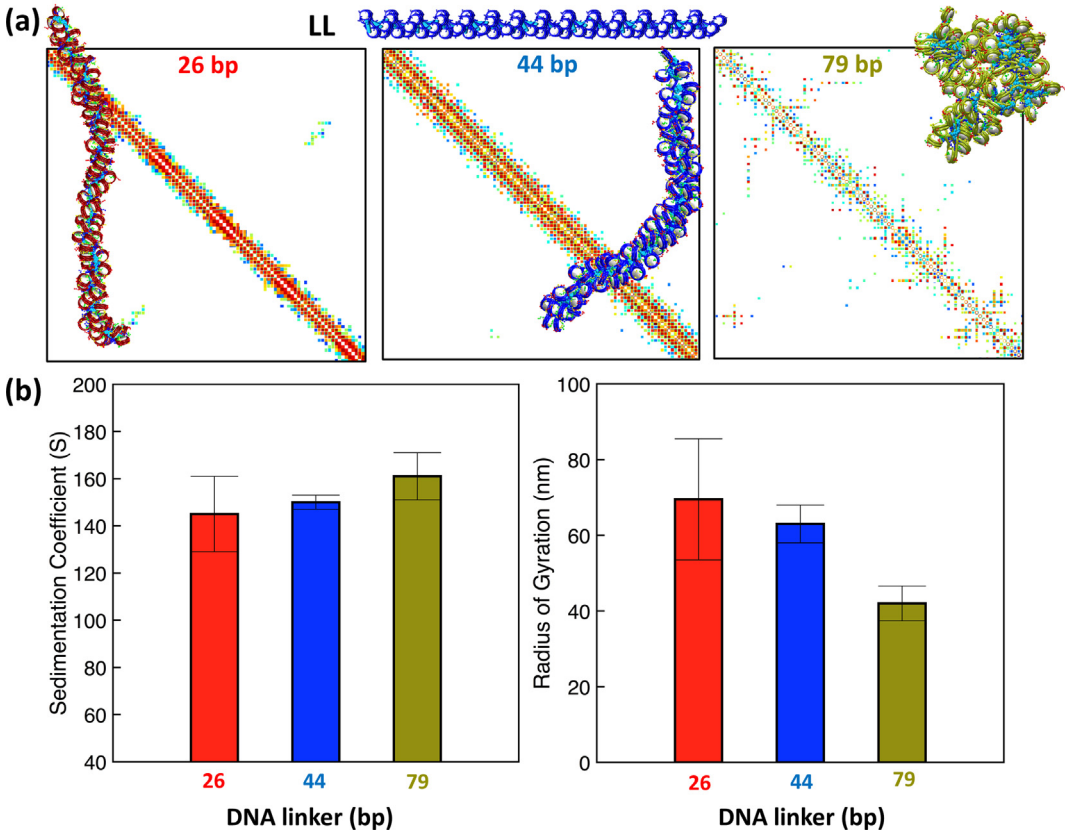

Figure 1. Equilibrated structural properties for uniform fibers with different DNA linker lengths without nucleosome free regions (NFRs) show different folding patterns but no discrete clutches. (a) Internucleosome interaction density matrices of representative uniform fibers with short (red), medium (blue), and long (green) linker lengths. Contact maps are determined by counting distances between any two nucleosome constituents (core or histone tails) that are within 2 nm. Representative structures for each system are shown on the corresponding contact map, and the initial structure for the fiber with medium LL is shown at top. (b) Global compaction parameters: sedimentation coefficient in Svedberg units (left) and radius of gyration in nm (right) for the chromatin fibers with short, medium, and long DNA linker lengths.

63 ± 5 nm in medium-linker fibers to 42 ± 5 nm in long-linker fibers. Consistent with these results, the sedimentation coefficient increases from 145 ± 16 S in short-linker fibers to 150 ± 3 S in the medium-linker fibers to 161 ± 10 S in the long-linker fibers (Figure 1(b)).

Overall, these results show that without NFRs, clutches do not form but the length of the DNA linker regulates chromatin architecture profoundly. As we have already shown, irregular linker lengths[72] or nucleosome free regions[47] encourage long-range internucleosome contacts through hierarchical looping.

NFRs produce discrete clutches

As NFRs are implicated in the regulation of gene expression,[18,73] we examine their effect in the context of uniform fibers by assigning short (114 bp), medium (220 bp), and long (326 bp) NFRs positioned every 10 nucleosomes. We consider all 9 combinations of short/medium/long DNA linker lengths and 114/220/326 bp NFRs. Figure 2(a) shows the computed average number of nucleosomes per clutch for each system, and (b) shows representative chromatin configurations for each system.

For all fibers, there is a pronounced decrease in the average number of nucleosomes per clutch when NFRs lengths increase from short to medium lengths. This decrease in clutch size is slightly less pronounced in systems with medium and long-linker DNA. The lower sensitivity to changes in NFRs lengths in fibers with longer linker DNA might result from a higher fiber flexibility, which allows the formation of larger clutches by long-range nucleosome interactions.

When NFRs are increased from medium to long lengths, we note a less pronounced effect for all systems, indicating that the effect of NFRs becomes limiting at medium lengths.

When NFRs are kept constant but the DNA linker lengths vary, the effect is more moderate than when DNA linker lengths are kept constant and NFRs lengths vary. Indeed, for the short NFRs systems, a clear trend of smaller clutch size with larger linker lengths can be observed (three tall histograms in Figure 2(a)). For medium and long NFRs, the clutch size is much less sensitive to the DNA linker length.

As we report in Table S2, the decrease in nucleosome clutch size is consistent with an opening of the chromatin fiber that occupies a larger volume, has a larger radius of gyration, smaller sedimentation coefficient, and smaller packing ratio.

Overall, these results show that short DNA linker lengths and short NFRs are advantageous for the formation of larger clutches and that the effect of NFRs is very strong. Moreover, the overall trends are not affected by changes in salt, such as consideration of Mg^{2+} (Figure S7).

Importantly, the large standard deviations observed in the calculation of the average number of nucleosomes per clutch reflect the diverse nucleosomes clutches present in each individual chromatin fiber, rather than a poor sampling. Figure S8 shows the analysis of standard deviation fluctuations as a function of sample size for two different systems, which indicates that such deviations are independent of the sample size.

Linker histone density regulates clutch size by compacting chromatin fibers

Using super-resolution microscopy, we previously showed that nucleosome clutches are smaller and less compact in mouse embryonic stem cells (mESC) than in somatic cells like neural progenitor cells (mNPC).[26] To gain insight into the role of LH on nucleosome clutch organization, we study the effect of LH density on clutch size and chromatin compaction.

Figure 3(a) shows the average number of nucleosomes per clutch and number of clutches for fibers with long linker DNA (79 bp) and medium NFRs (220 bp) without LH (–LH) and with a density of 0.25, 0.50, 0.75, and 1 LH molecule per nucleosome. We see that nucleosome clutch size increases with the LH density. In particular, the size of the clutches increases from an average of 8 without LH to 19 in the fibers saturated with LH. Consistent with larger clutches, the number of clutches decreases from an average of 11 without LH to 6 in LH-saturated fibers. As we see from the chromatin fiber configurations in Figure 3(b), LH density has an important role in compacting the fibers, in agreement with previous results.[52,56,74] Indeed, the sedimentation coefficient of the fibers increases from 90 ± 11 S without LH to 119 ± 13 S in the LH-saturated system (Figure 3(b)). Supplementary video shows the folding of the fibers with different LH densities with nucleosomes colored based on the clutch they belong to. These trends are overall maintained when the fibers are modeled in divalent ion conditions (Figure S7). However, because both linker histones and divalent ions condense the fibers, the combined effect is not cumulative because of a physical limit on compaction.

To determine if the effect of LH density depends on the length of linker DNA and NFRs, we study a chromatin fiber with short DNA linker lengths (26 bp) and short NFRs (114 bp). Figure S9 shows the average number of nucleosomes per clutch for this fiber studied without LH and with 0.5 and 1 LH per nucleosome. Results show a similar overall increase in clutch size with the LH density as in the fiber with long DNA linker lengths and medium NFRs (Figure 3(a)).

Overall, our results on LH density confirm the important role of LH in chromatin compaction and

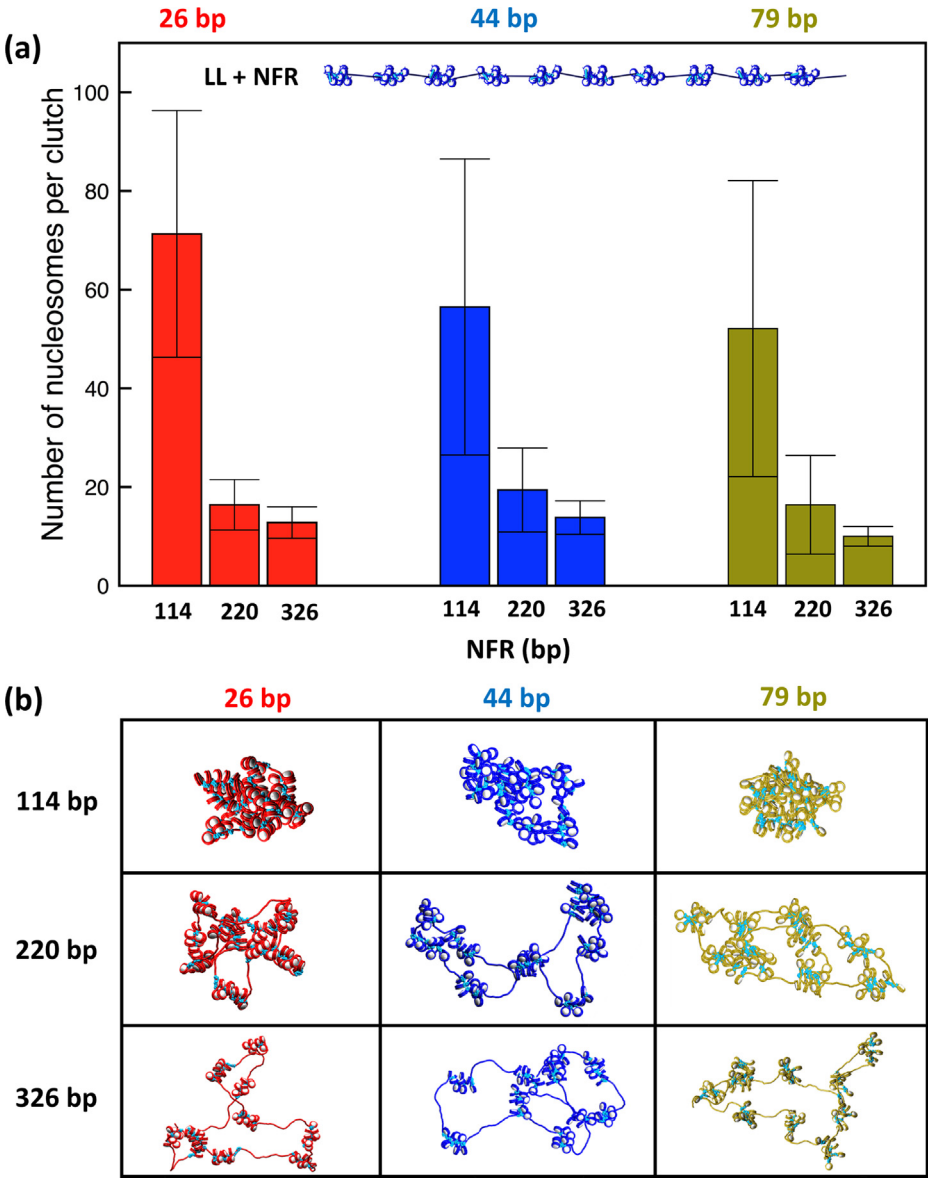

Figure 2. Equilibrated structural properties for uniform fibers with different DNA linker lengths and nucleosome free regions (NFRs) show dominance of NFR size in resulting nucleosome clutches. (a) Average number of nucleosomes per clutch for uniform fibers with short (red), medium (blue), and long (green) DNA linker lengths with short, medium, and long NFRs. At top shown is the initial configuration for the fiber with linker DNAs of 44 bp and NFRs of 220 bp. (b) Representative fiber configurations for each system, with LHs shown in cyan.

provide further insight on the associated clutch pattern mechanisms.

Acetylation levels moderately affect nucleosome clutches

Recently, we showed that the DNA compaction inside nucleosome clutches is affected by histone tail acetylation, which might result from the disruption of the nucleosome/DNA interaction upon acetylation.[34] To further study the effect of acetylation on nucleosome clutches, we simulate fibers with short DNA linker lengths (26 bp) and 5 short NFRs (114 bp) without acetylation and with 25, 50, 75, and 100% of tails acetylated.

Figure 4(a) shows the average number of nucleosomes per clutch at different acetylation levels. The corresponding chromatin fiber structures are shown in Figure 4(b). We see that the average number of nucleosomes per clutch decreases as Ac levels increase. In fibers without acetylated tails, most of the nucleosomes are close to one another, producing an average of 89 nucleosomes per clutch. On the other extreme,

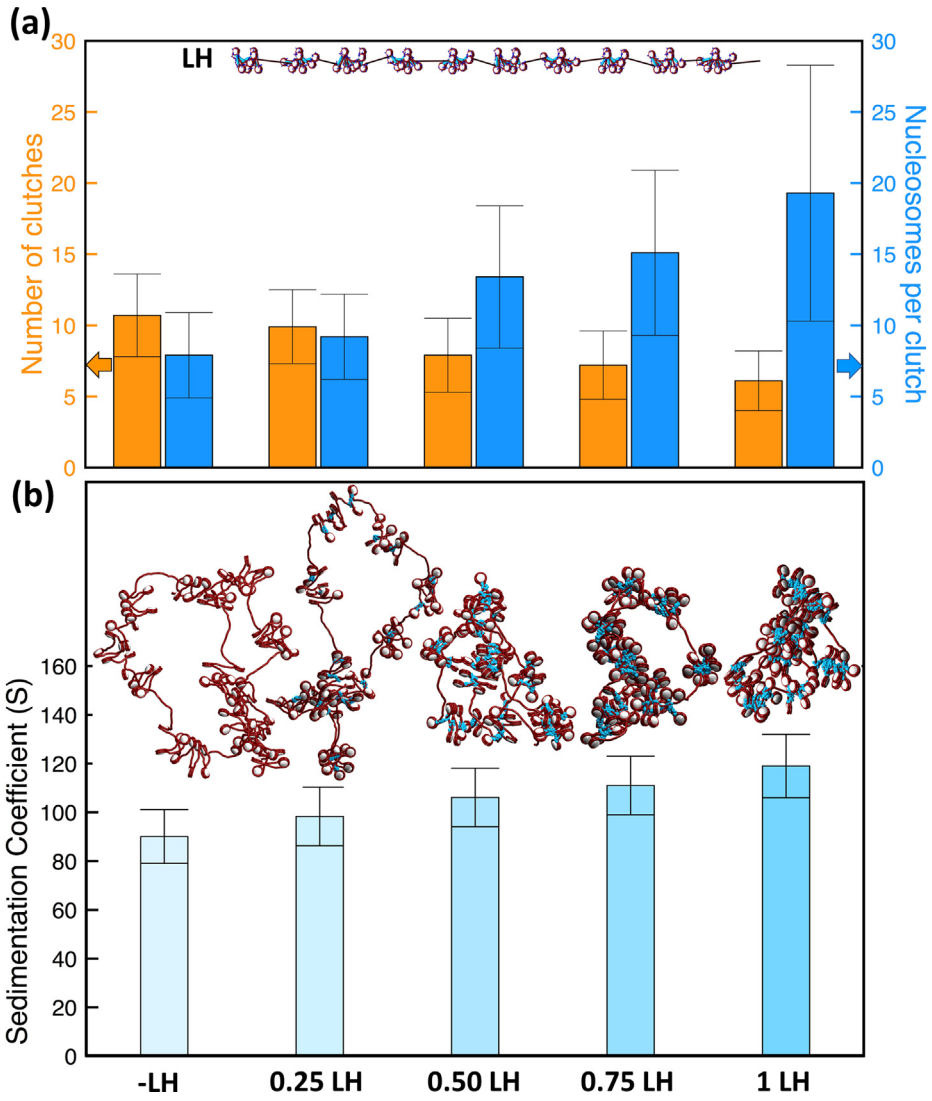

Figure 3. Equilibrated structural properties for different linker histone (LH) density show clutch size compaction effect. (a) Average number of clutches (left axis, orange bars) and average number of nucleosomes per clutch (right axis, blue bars) for the fiber with long DNA linker (79 bp) and medium NFRs (220 bp) simulated with different LH densities. From left to right: chromatin fiber without LH (–LH), with 0.25 LH per nucleosome (0.25 LH), 0.5 LH per nucleosome (0.5 LH), 0.75 LH per nucleosome (0.75 LH), and 1 LH per nucleosome (1 LH). At top shown is the starting configuration for the system with 0.5 LH per nucleosome. (b) Sedimentation coefficient for each LH density. Representative fibers for each condition are shown, with LHs in cyan.

when 100% of tails are acetylated, the average number of nucleosomes per clutch is 58. The fiber configurations and radii of gyration (Figure 4 (b)) show how acetylation of the histone tails triggers chromatin unfolding, thereby decreasing the size of nucleosome clutches. As can be seen in Figure S7, this trend is sensitive to the presence of Mg^{2+}. As the effects of Mg^{2+} and acetylation are opposite on fiber compaction, there is no overall decrease in the number of nucleosomes per clutch when acetylation levels increase at divalent ion conditions.

In Figure 5, we further analyze the interactions established between each H2A, H2B, H3, and H4 tail and other chromatin elements, such as the parental core, parental DNA, non-parental core, non-parental DNA, and other tails. The frequencies of such interactions indicate that when tails are acetylated, interactions between H4 tails and non-parental cores significantly decrease (Figure 5(a)). On the other hand, interactions between the tails and the parental core (Figure 5(b)) and parental DNA (Figure 5(c)) increase. There is also a commensurate increase in the interaction between tails of histones H2A and H3 with non-parental DNA and decrease of the interaction between H2B and non-parental DNA (Figure 5(d)). Finally, the interactions among tails also decrease when they are acetylated (Figure 5(e)). In general, acetylated tails interact

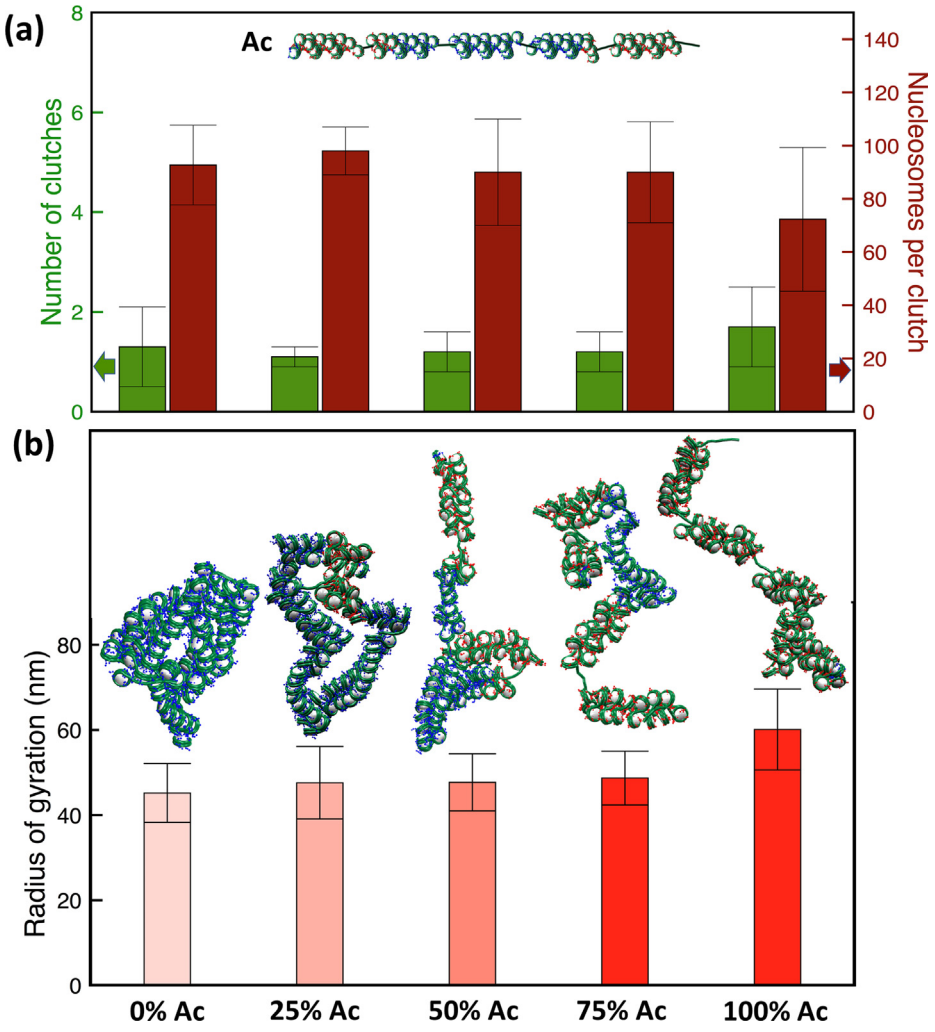

Figure 4. Equilibrated structural properties of acetylated fibers show that acetylation (Ac) levels modulate clutch patterns by unfolding chromatin. a) Average number of clutches (left axis, green bars) and average number of nucleosomes per clutch (right axis, dark red bars) for the fiber with short DNA linker (26 bp) and short NFRs (114 bp) simulated with different Ac levels from 0 to 100%. At top shown is the starting configuration for the system with 50% of tails acetylated. b) Radius of gyration for each acetylation level. Representative fibers for each condition are shown, with native tails in blue and acetylated tails in red.

less with other chromatin elements, as shown by the increase of free tails frequency (Figure 5(f)). Overall, these results indicate that chromatin unfolding and reduction of nucleosome clutch size upon acetylation occur due to a loss of nucleosome/nucleosome interactions. Figure S10 compares the internucleosome interaction contact maps for a fiber without acetylation and a fiber with 100% tails acetylated, showing the loss of short and medium-range interactions upon acetylation.

We have previously showed that histone tails are implicated in directing chromatin folding at the nucleosome level.[75] They establish segregated interactions in which nucleosomes of the same type (i.e., nucleosomes with native tails) cluster together and separately from nucleosomes of other type (i.e., nucleosomes with acetylated tails). As observed in the fiber configurations for the system with 25% and 75% of tails acetylated (Figure 4(b)), we see this domain segregation in which acetylated tails (red) cluster together, while native tails (blue) cluster separately.

When we study the same fiber but with 10 NFRs instead of 5 (Figure S11(a)), and the fiber with long DNA linker lengths (79 bp) and 10 medium NFRs (220 bp) (Figure S11(b)), we see that acetylation levels do not significantly affect the size of nucleosome clutches, indicating that the effect of NFRs dominates over the effect of acetylation.

Overall, our results show a moderate effect of histone tail acetylation on the regulation of nucleosome clutches. This effect depends on the length of DNA linker and NFRs, and on the number of NFRs. Because our model does not

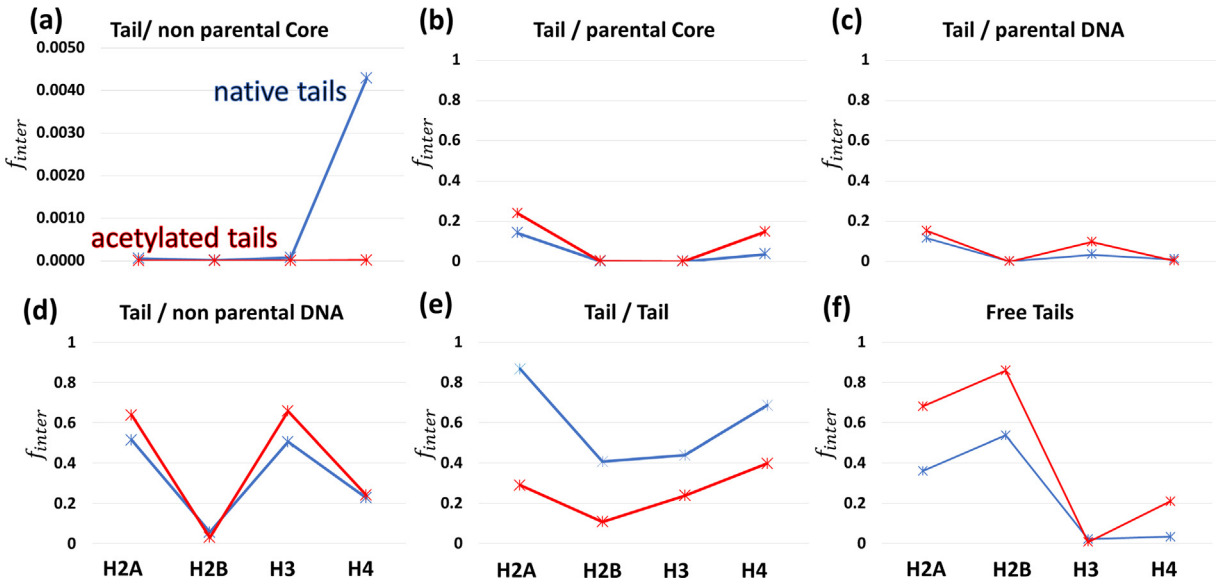

Figure 5. Tail interaction frequencies for 100% acetylated fiber and native fiber with short DNA linker length (26 bp) and 5 short NFRs (114 bp). Interaction frequencies (f_{inter}) are calculated by measuring the fraction of Monte Carlo steps in which each tail is within 2 nm of a non-parental Core (a), a parental Core (b), parental DNA (c), non-parental DNA (d), or tails of a different nucleosome (e). We also calculate the fraction of MC steps that each tail is not interacting with any other chromatin element (f). Interactions are calculated along the 2000 configurations ensemble for each system and normalized by the total number of configurations.

account for nucleosome sliding or explicit nucleosome/DNA interaction, further implications of histone tails acetylation cannot be made.

Designed fibers with predicted folding and nucleosome clutches

Now, we "design" chromatin fibers *in silico* to produce target clutch patterns using what we learned above from the effect of various parameters on clutch behavior.

Specifically, we design three types of fibers as detailed in Methods (Section '*Design of fibers with naturally-occurring DNA linker lengths*') and illustrated in Figure 6: (1) fiber with one large and one small clutch, (2) pearl necklace-like fiber with equally spaced nucleosome clutches, (3) fiber with clutches of variable sizes. For all these 3 designs we use the Voong distribution of DNA linker lengths.[17]

To obtain the large clutch in the first design (Figure 6, Design 1), we promote hierarchical looping (Figure S12) by using low LH density, such as found in metaphase chromatin.[70] We distribute LHs in three groups of nucleosomes (Methods, Section '*Design of fibers with naturally-occurring DNA linker lengths*') and produce two LH-depleted regions located between the three groups. The LH-depleted regions induce hierarchical looping, merging two groups of nucleosomes and producing the large clutch. To produce the small clutch, we promote chromatin segregation. We further acetylate the LH-depleted regions (Methods, Section '*Design of fibers with naturally-occurring DNA linker lengths*') that border one of the groups of nucleosomes with native tails and LH. The nucleosomes in the acetylated-rich regions interact with one another and separate from nucleosomes with native tails. We also prescribe short NFRs (5 of 114 bp and 4 of 167 bp) positioned before and after the small clutch to separate it from the large clutch.

To design the pearl necklace-like construct (Figure 6, Design 2), we use high LH density and medium NFRs between groups of 4 nucleosomes. The presence of 1 LH per nucleosome stabilizes each individual group of nucleosomes.

To create variable-sized clutches (Figure 6, Design 3), we promote heterogeneity by placing groups of nucleosomes of different sizes (3, 7, 8, 9, 11, and 12 nucleosomes) along the fiber. We spread them out using short and long NFRs (Methods, Section '*Design of fibers with naturally-occurring DNA linker lengths*'). We omit LH to discourage compaction, as well as acetylation to avoid segregation.

Overall, we see that it is possible to anticipate how clutches in a chromatin fiber form based on the distribution of NFRs, LH density, and acetylation levels. Other epigenetic factors likely have characteristic effects as well.

Regulation of nucleosome clutches in gene-encoding fibers

To understand how all the factors contribute to gene structure, we study the effect of different LH

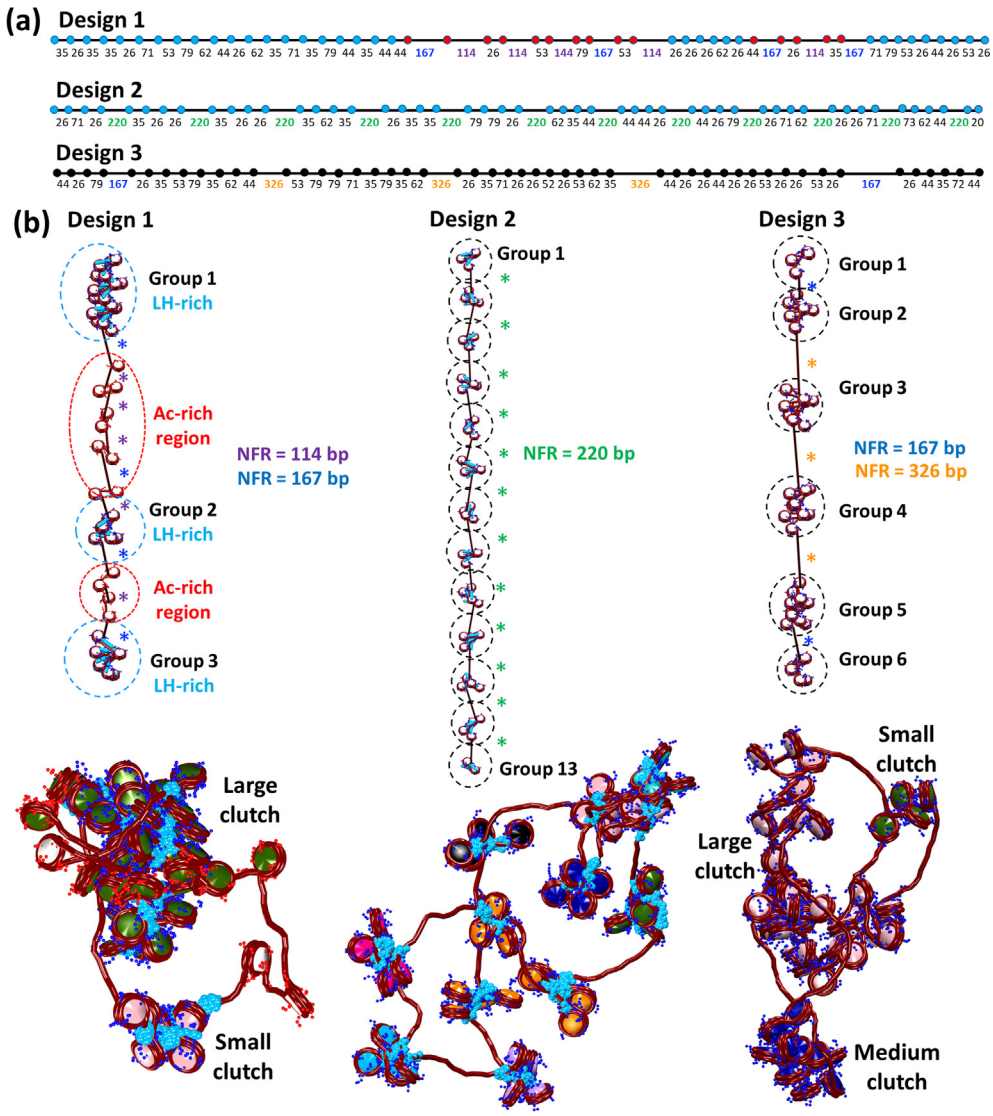

Figure 6. Designed fibers with specific clutch patterns. (a) Molecular sketches showing the fiber configurations for each 50-nucleosome chromatin design. Values for DNA linker lengths (black) and NFRs (blue, violet, green, and orange) are specified. Blue circles represent nucleosomes with LH, red circles acetylated (Ac) nucleosomes, and black circles nucleosomes without LH or Ac. (b) Top: initial configuration for each designed fiber with LH-rich regions denoted by cyan circles, Ac-rich regions by red circles, groups of nucleosomes by dashed black circles, and NFRs by asterisks. Bottom: equilibrated configurations for each designed fiber with nucleosomes colored based on the clutch they belong to, acetylated tails red, native tails blue, and linker histones cyan.

densities and acetylation levels on two specific genes, the human HOXC gene locus and the mouse Pou5f1 locus. When studying LH density effects, we maintain nucleosome positions and acetylation levels and positions as in the native HOXC and Pou5f1 genes.[46,47] Similarly, we maintain nucleosome positions and LH density and positions as in the native HOXC and Pou5f1 genes[46–47] when investigating acetylation level effects.

Figure 7(a) shows the average number of nucleosomes per clutch for the HOXC gene without LH and with 0.5 and 1 LH molecule per nucleosome, along with representative fiber configurations for each system. Similar to the trends in the uniform fiber (Figure 3), higher LH densities increase the size of the nucleosome clutches. The chromatin fiber configurations in Figure 7(a) and sedimentation coefficients (Table S3) show that in HOXC, as well as in uniform fibers, LHs globally compact chromatin fibers, favoring the formation of larger nucleosome clutches. For reference, we indicate the average number of nucleosomes per clutch for the native HOXC, calculated by analyzing the trajectories of our previous study.[47] Native HOXC has an LH density of 0.2 LH per nucleosome and LHs are positioned based on mouse embryonic stem cells data[49] (Table S1). We see that the

native HOXC gene follows well the trend observed for the different LH densities, with an average nucleosome clutch size that lies in between the system without LH and with 0.5 LH per nucleosome. When the LH density increases from 0 to 1 LH per nucleosome, the clutch size increases 2.5 times fold, similar to the increase of 2.4 times observed in the uniform fiber (Figure 3(a)).

When we explore histone tail acetylation, contrary to the effect observed for uniform fibers (Figure 4), we see that the fibers become more globular as acetylation levels increase. Nucleosomes appear to be closer to one another, so that the average number of nucleosomes per clutch increases as acetylation levels saturate (Figure 7(b)). Moreover, the sedimentation coefficient of the fiber increases (Table S3) and the fiber volume decreases upon acetylation (Table S3), compatible with a more globular structure. Similar to the trend observed for different LH densities, the average number of nucleosomes per clutch for the native HOXC gene, which contains 30% of tails acetylated, lies between values for the fiber without acetylated tails and the fiber with 50% of tails acetylated.

The effect of acetylation appears to depend on the specific fiber configuration. In fibers with few, short NFRs, chromatin unfolding occurs upon acetylation due to disruption of nucleosome/nucleosome interactions, as we have observed before for fibers without NFRs.[35] On the other hand, in fibers with more NFRs, even though inter-nucleosome interactions are disrupted, NFRs allow folding into higher-order structures, which in turn increase clutch size. This effect could result from the combination of chromatin segregation and high flexibility induced by NFRs. To further characterize the effect of acetylation on nucleosome clutches, we measure clutch compaction as the number of nucleosomes per clutch area. Even though clutches appear to be larger upon acetylation, their compaction decreases (Table S3), in agreement with the fiber structures showing larger but less compact clutches upon acetylation (Figure 7(b)).

Figure 8 shows the average number of nucleosomes per clutch for the Pou5f1 gene studied with different linker histone densities and acetylation levels. When studying LH density (Figure 8(a)), we see that higher LH densities decrease clutch size. This is attributed to a more

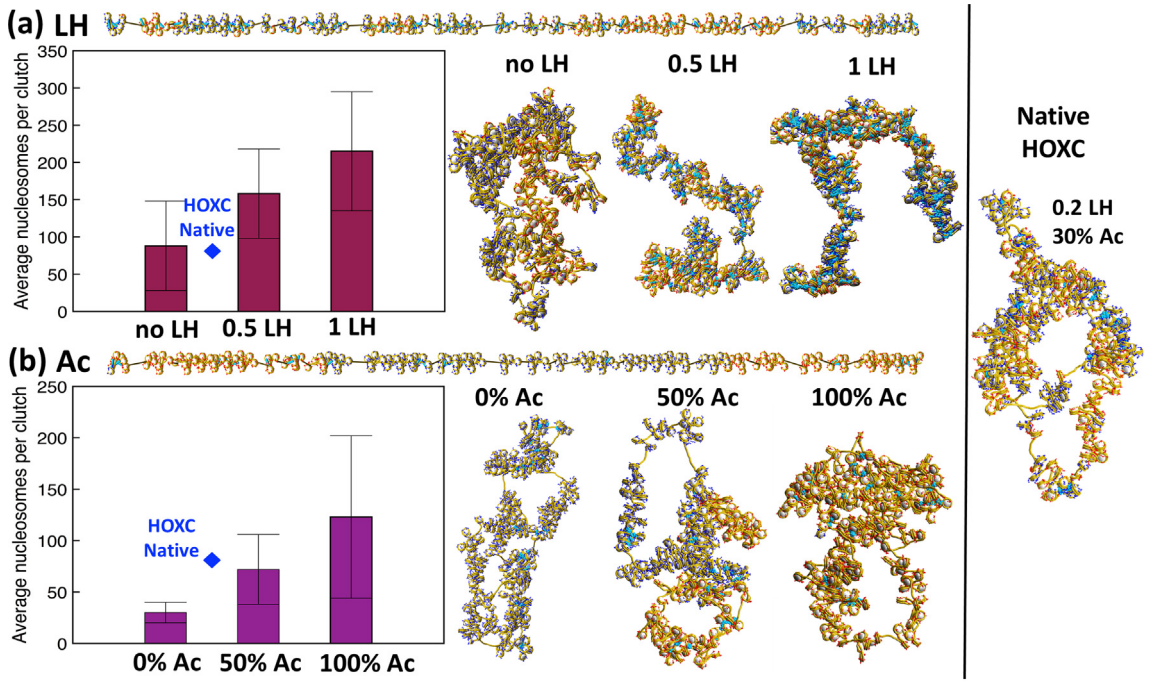

Figure 7. Properties for HOXC gene show that linker histone (LH) density and acetylation (Ac) levels control nucleosome clutches of the gene. (a) Average number of nucleosomes per clutch for HOXC without LH and with 0.5 and 1 LH per nucleosome. At top shown is the initial configuration for the system with 0.5 LH per nucleosome. At right are shown the equilibrated structures for each LH density. LHs are shown in cyan. (b) Average number of nucleosomes per clutch for HOXC without Ac and with 50% and 100% of tails acetylated. At top shown is the initial configuration for the system with 50% of tails acetylated. At right are shown the equilibrated structures for each acetylation level. Native tails are shown in blue and acetylated tails in red. In both plots, the blue diamond indicates the value for the native HOXC obtained by analyzing the simulations of our previous work.[47] The native HOXC has a LH density of 0.2 and LHs positioned based on data for mouse embryonic stem cells[49] and an acetylation level of 30% with acetylation islands positioned based on Chip-seq data.[47] A representative structure of native HOXC is also shown.

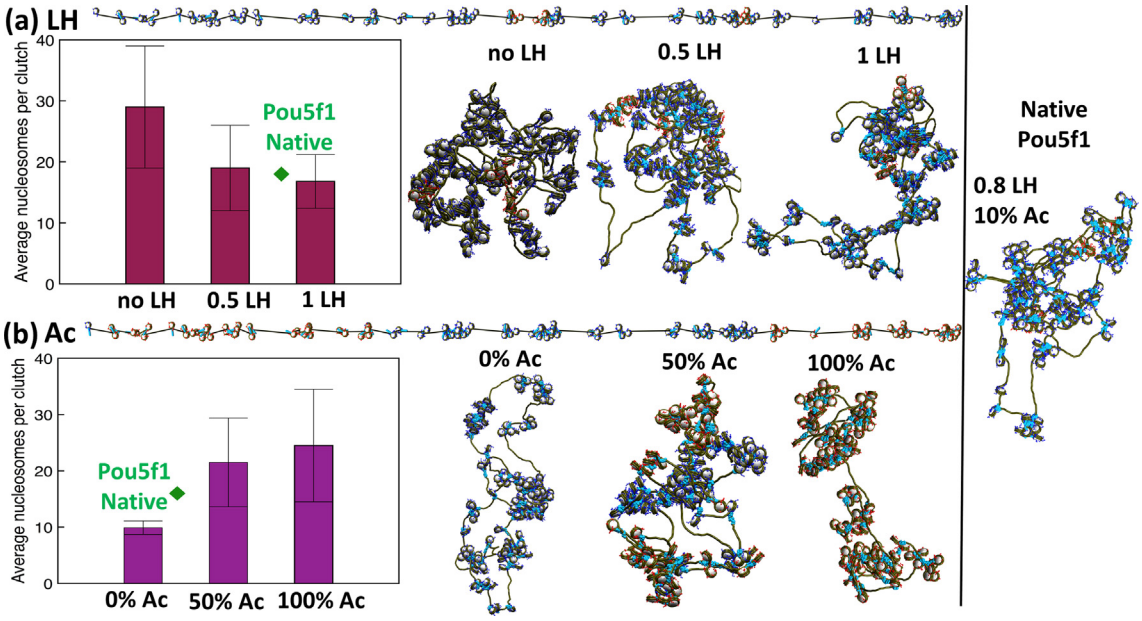

Figure 8. Properties of the Pou5f1 gene show that linker histone (LH) density and acetylation (Ac) levels control nucleosome clutches of the gene. (a) Average number of nucleosomes per clutch for Pou5f1 system without LH and with 0.5 and 1 LH per nucleosome. At top shown is the initial configuration for the system with 0.5 LH per nucleosome. At right are shown representative structures for each LH density. LHs are shown in cyan. (b) Average number of nucleosomes per clutch for Pou5f1 system without Ac and with 50% and 100% of tails acetylated. At top shown is the initial configuration for the system with 50% of tails acetylated. At right are shown equilibrated structures for each acetylation level. Native tails are shown in blue and acetylated tails in red. In both plots, the green diamond indicates the value for the native Pou5f1 previously determined[47] that has a LH density of 0.8 and an acetylation level of 10%. A representative structure of the native Pou5f1 is also shown.

globular structure in the fiber without LHs, which favors nucleosomes to be close to one another. Consistently, there is an increase in the radius of gyration as LH density increases (Table S4). These results are in agreement with our previous study showing that low LH densities, such as in metaphase chromosomes, can trigger hierarchical looping, promoting a more flexible, looped, and globular structure.[70] Even though nucleosome clutches become smaller when LH density increases, their compaction slightly increases (Table S4). Similarly, when acetylation levels increase, the size of nucleosome clutches increase (Figure 8(b)), commensurate with the structure becoming more globular (Table S4). However, as in the HOXC system, their compaction decreases (Table S4).

Overall, we see that, in general, in gene-encoding fibers, LH density and Ac levels produce more compact and less compact clutches, respectively, with details that depend on the specific fiber configuration.

Discussion

In this article, we use our nucleosome-resolution chromatin mesoscale model to dissect nucleosome clutch patterns in kb chromatin fibers (Figure 9). We study clutches in uniform, non-uniform, and gene-encoding fibers, and focus on their regulation by nucleosome positions, linker histone density, and acetylation levels.

Our studies on uniform fibers reveal that nucleosome positions prominently regulate chromatin folding patterns. In general, shorter linker DNA and/or shorter nucleosome free regions (NFRs) favor more compact fibers with larger nucleosome clutches. In Nature, the average nucleosome repeat length (NRL) is tightly regulated and varies among organisms,[6,41] cell types,[76] and along cell stages.[9,32] NFRs are also regulated by multiple factors, such as properties of the DNA,[77] transcriptional factors,[78] and chromatin regulators.[79] Moreover, it has been shown that nucleosome positions, alone, can dictate chromatin folding and interacting domains in yeast.[80] Thus, by regulating nucleosome positions, the cell machinery can determine the size of nucleosome clutches and levels of compaction. Whereas shorter DNA linker lengths are related to high transcriptional activity, longer NFRs are thought to facilitate the initiation of transcription. The NFRs in particular are crucial for defining segregated domains and hence clutch patterns. However, linker histones, posttranslational modifications, and binding of proteins also regulate

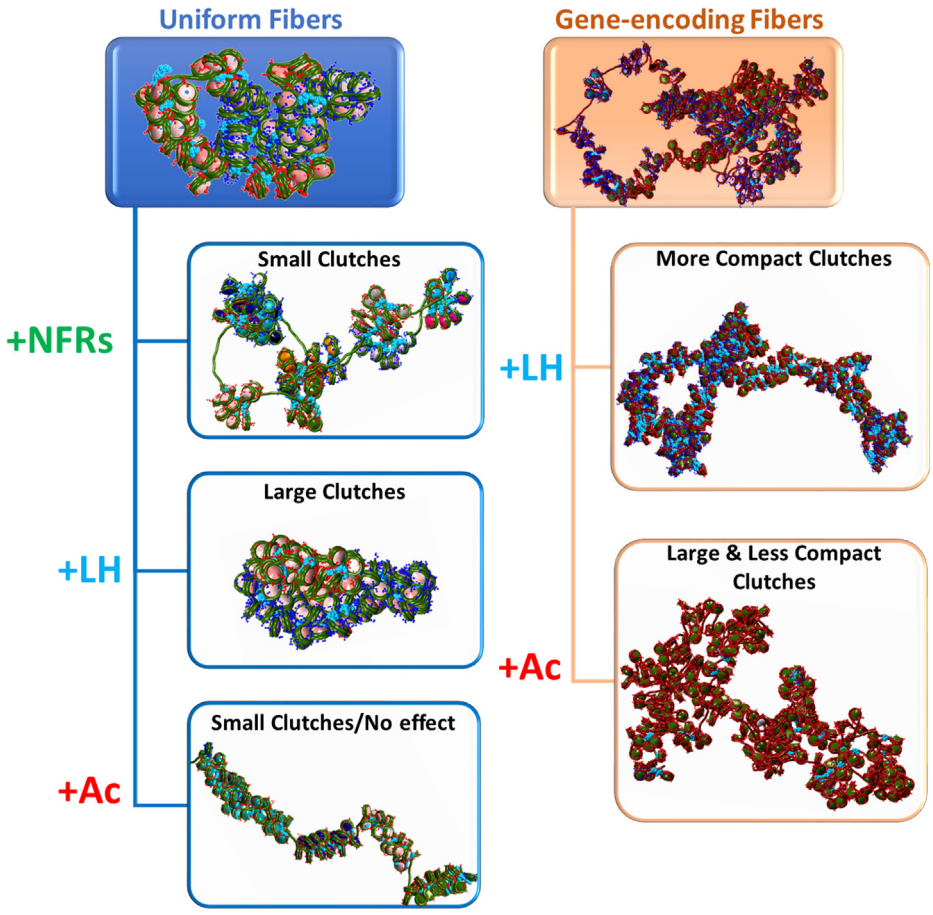

Figure 9. Simplified scheme summarizing key findings. In uniform fibers (left, blue boxes), NFRs are necessary to establish clutches, and longer NFRs produce smaller clutches. Higher LH density produces larger clutches through a chromatin compaction mechanism. Higher Ac levels produce smaller clutches through a chromatin unfolding mechanism, although this effect strongly depends on the fiber configuration. For some fibers, increasing Ac levels do not affect nucleosome clutches. For gene-encoding fibers (right, orange boxes), higher LH density produces larger or smaller clutches, but these clutches are more compact. Higher Ac levels produce larger and less compact clutches.

clutch patterns and chromatin global folding. As we show for the systems studied with different LH densities and Ac levels, if NFRs are kept constant while other parameters vary, nucleosome clutches are affected. In systems where LH density and Ac levels favor a highly compact fiber, the presence of NFRs might not be sufficient to lead to formation of clutches. A delicate balance among all these parameters is important for achieving the chromatin fiber architecture on both global and local levels.

Beyond regulating chromatin compaction, LHs have additional important functions, such as epigenetic regulation[52] and regulation of genomic functions such as DNA replication and repair.[4] Our studies on uniform fibers show that through compacting the fibers, LHs affect clutch patterns, increasing the size of clutches. As we reported previously,[26] somatic cells have larger and more compact clutches than pluripotent cells. As somatic cells have higher LH density than pluripotent cells,[6] our results indicate that in somatic cells, a high LH density could help produce larger nucleosome clutches by compacting the chromatin fiber, whereas in pluripotent cells, a low LH density could favor the formation of open chromatin with smaller nucleosome clutches, activating transcriptional activity.[81] In agreement with this, some genomic regions, such as promoters of highly transcribed genes, have a low LH density, whereas regions with silenced chromatin are enriched with LHs.[4] Moreover, it has been reported that a reduction of LH density leads to a shortening of the linker DNA[6] and that the combination of both parameters is important in determining chromatin fiber structure.[82] Thus, the balance between nucleosome positions and LH density could help regulate nucleosome clutches.

Histone acetylation is well known to promote gene transcription by decompacting the chromatin fiber and making the DNA more accessible to the transcriptional machinery.[36,83,84] Recently, we showed that DNA/nucleosome interactions are affected by histone acetylation through reduction of clutch-associated DNA.[34] Our studies on acety-

lation levels in uniform fibers show that acetylation triggers chromatin unfolding and reduces nucleosome clutches size moderately. However, this effect depends on the fiber configuration. In fibers with more NFRs or longer linker DNAs and NFRs, no significant effect is observed.

It has been shown that acetylation levels increase in pluripotent cells, compared to somatic cells.[85] Thus, higher acetylation levels in these cells could help produce smaller or less compact clutches, which in turn increase the accessibility to DNA and favor gene transcription. Depending on acetylation locations, different dynamic events like unwrapping or disassembly may occur.[86] Both events could reduce the size of nucleosome clutches or the clutch-associated DNA.[34] Though our model does not account for such nucleosome dynamics, it is clear that clutch regulation due to the disruption of nucleosome/nucleosome interactions from histone tail acetylation plays a role.

When we apply what we learned from uniform fibers to the design of non-uniform fibers, we see that it is possible to design clutch patterns with specific combinations of nucleosome positions, LH density, and Ac levels. Clearly, in gene-encoding fibers, clutch patterns are more intricate.

Our studies on the HOXC and Pou5f1 genes indicate that LH density and Ac levels can be applied to modulate chromatin architecture on global and local levels. In general, higher LH density produces more compact clutches, while higher Ac levels produce less compact clutches.

In a recent study, we explore clutch formation in chromatin fibers typical of mouse embryonic stem cells and neural progenitor cells that vary in nucleosome positions, LH density, and acetylation levels.[46] We observed that clutches were larger and more compact in somatic cells, in agreement with our previous experimental results.[26] Based on the present results, we conclude that the mechanism regulating nucleosome clutches during cell differentiation, and possibly related cellular processes, reflects a delicate balance of factors arising from nucleosome positions, LH densities, and epigenetic marks. Other mechanisms like binding of regulatory proteins and various epigenetic modifications may also be involved. Further studies of such factors on chromatin structure at the nucleosome, fiber, and gene levels could further illuminate these important aspects of genome regulation.

credit authorship contribution statement

Stephanie Portillo-Ledesma: Conceptualization, Investigation, Methodology, Writing - original draft. **Lucille H. Tsao:** Conceptualization, Investigation, Editing - original draft. **Meghna Wagley:** Formal analysis, Software. **Melike Lakadamyali:** Conceptualization, Editing - original draft. **Maria Pia Cosma:** Conceptualization, Editing - original draft. **Tamar Schlick:** Conceptualization, Writing - original draft, Funding acquisition, Supervision.

Acknowledgements

Support from the National Institutes of Health, National Institutes of General Medical Sciences Awards R01GM055264 and R35-GM122562, National Science Foundation RAPID Award (2030377) from the Division of Mathematical Sciences, and Philip-Morris USA Inc. and Philips-Morris International to T.S. are gratefully acknowledged.

Declaration of Competing Interest

The authors declare that they have no known competing financial interests or personal relationships that could have appeared to influence the work reported in this paper.

Appendix A. Supplementary material

Supplementary data to this article can be found online at https://doi.org/10.1016/j.jmb.2020.11.001.

Received 10 August 2020;
Accepted 2 November 2020;
Available online xxxx

Keywords:
nucleosome clutches;
mesoscale modeling;
nucleosome positions;
linker histone density;
histone acetylation levels

† These authors equally contributed to this work.

Abbreviations:
Ac, acetylation; bp, base pairs; DBSCAN, Density-based clustering algorithm; LH, linker histone; LLs, linker lengths; MNase-seq, micrococcal nuclease sequencing; MC, Monte Carlo; mESC, mouse embryonic stem cells; NPC, neural progenitor cells; NFRs, nucleosome free regions; NRL, nucleosome repeat length

References

1. Cutter, A.R., Hayes, J.J., (2015). A brief review of nucleosome structure. *FEBS Lett.*, **589**, 2914–2922. https://doi.org/10.1016/j.febslet.2015.05.016.
2. Zhou, K., Gaullier, G., Luger, K., (2019). Nucleosome structure and dynamics are coming of age. *Nat. Struct. Mol. Biol.*, **26**, 3–13. https://doi.org/10.1038/s41594-018-0166-x.
3. Happel, N., Doenecke, D., (2009). Histone H1 and its isoforms: contribution to chromatin structure and function.

Gene., **431**, 1–12. https://doi.org/10.1016/j.gene.2008.11.003.

4. Fyodorov, D.V., Zhou, B.-R., Skoultchi, A.I., Bai, Y., (2018). Emerging roles of linker histones in regulating chromatin structure and function. *Nat. Rev. Mol. Cell. Biol.*, **19**, 192–206. https://doi.org/10.1038/nrm.2017.94.
5. Widom, J., (1998). Chromatin structure: Linking structure to function with histone H1. *Curr. Biol.*, **8**, R788–R791.
6. Woodcock, C.L., Skoultchi, A.I., Fan, Y., (2006). Role of linker histone in chromatin structure and function: H1 stoichiometry and nucleosome repeat length. *Chromosom. Res.*, **14**, 17–25. https://doi.org/10.1007/s10577-005-1024-3.
7. Bates, D.L., Thomas, J.O., (1981). Histories H1 and H5: one or two molecules per nucleosome?. *Nucleic Acids Res.*, **9**, 5883–5894.
8. Popova, E.Y., Grigoryev, S.A., Fan, Y., Skoultchi, A.I., Zhang, S.S., Barnstable, C.J., (2013). Developmentally regulated linker histone H1c promotes heterochromatin condensation and mediates structural integrity of rod photoreceptors in mouse retina. *J. Biol. Chem.*, **288**, 17895–17907. https://doi.org/10.1074/jbc.M113.452144.
9. Fan, Y., Nikitina, T., Zhao, J., Fleury, T.J., Bhattacharyya, R., Bouhassira, E.E., Stein, A., Woodcock, C.L., et al., (2005). Histone H1 depletion in mammals alters global chromatin structure but causes specific changes in gene regulation. *Cell.*, **123**, 1199–1212. https://doi.org/10.1016/j.cell.2005.10.028.
10. Healton, S.E., Pinto, H.D., Mishra, L.N., Hamilton, G.A., Hamilton, G.A., Wheat, J.C., Swist-Rosowska, K., Shukeir, N., et al., (2020). H1 linker histones silence repetitive elements by promoting both histone H3K9 methylation and chromatin compaction. *Proc. Natl. Acad. Sci. U. S. A.*, **117**, 14251–14258. https://doi.org/10.1073/pnas.1920725117.
11. Struhl, K., Segal, E., (2013). Determinants of nucleosome positioning. *Nat. Struct. Mol. Biol.*, **20**, 267–273. https://doi.org/10.1038/nsmb.2506.
12. Yigit, E., Zhang, Q., Xi, L., Grilley, D., Widom, J., Wang, J.-P., Rao, A., Pipkin, M.E., (2013). High-resolution nucleosome mapping of targeted regions using BAC-based enrichment. *Nucleic Acids Res.*, **41**, e87. https://doi.org/10.1093/nar/gkt081.
13. Schwarzbauer, K., Bodenhofer, U., Hochreiter, S., (2012). Genome-wide chromatin remodeling identified at GC-rich long nucleosome-free regions. *PLoS One*, **7** https://doi.org/10.1371/journal.pone.0047924. e47924–e47924.
14. Albert, I., Mavrich, T.N., Tomsho, L.P., Qi, J., Zanton, S.J., Schuster, S.C., Pugh, B.F., (2007). Translational and rotational settings of H2A.Z nucleosomes across the Saccharomyces cerevisiae genome. *Nature*, **446**, 572–576. https://doi.org/10.1038/nature05632.
15. Brogaard, K., Xi, L., Wang, J.-P.P., Widom, J., (2012). A map of nucleosome positions in yeast at base-pair resolution. *Nature*, **486**, 496–501. https://doi.org/10.1038/nature11142.
16. Moyle-Heyrman, G., Zaichuk, T., Xi, L., Zhang, Q., Uhlenbeck, O.C., Holmgren, R., Widom, J., Wang, J.-P., (2013). Chemical map of Schizosaccharomyces pombe reveals species-specific features in nucleosome positioning. *Proc. Natl. Acad. Sci.*, **110**, 20158–20163. https://doi.org/10.1073/pnas.1315809110.
17. Voong, L.N., Xi, L., Sebeson, A.C., Xiong, B., Wang, J.-P., Wang, X., (2016). Insights into nucleosome organization in mouse embryonic stem cells through chemical mapping. *Cell*, **167**, 1555–1570.e15. https://doi.org/10.1016/j.cell.2016.10.049.
18. Radman-Livaja, M., Rando, O.J., (2010). Nucleosome positioning: how is it established, and why does it matter?. *Dev. Biol.*, **339**, 258–266. https://doi.org/10.1016/j.ydbio.2009.06.012.
19. Zhang, W., Li, Y., Kulik, M., Tiedemann, R.L., Robertson, K.D., Dalton, S., Zhao, S., (2016). Nucleosome positioning changes during human embryonic stem cell differentiation. *Epigenetics*, **11**, 426–437. https://doi.org/10.1080/15592294.2016.1176649.
20. Deniz, Ö., Flores, O., Aldea, M., Soler-López, M., Orozco, M., (2016). Nucleosome architecture throughout the cell cycle. *Sci. Rep.*, **6**, 19729.
21. Nocetti, N., Whitehouse, I., (2016). Nucleosome repositioning underlies dynamic gene expression. *Genes Dev.*, **30**, 660–672. https://doi.org/10.1101/gad.274910.115.
22. Kaplan, N., Moore, I.K., Fondufe-Mittendorf, Y., Gossett, A. J., Tillo, D., Field, Y., LeProust, E.M., Hughes, T.R., et al., (2009). The DNA-encoded nucleosome organization of a eukaryotic genome. *Nature*, **458**, 362–366. https://doi.org/10.1038/nature07667.
23. Fussner, E., Ching, R.W., Bazett-Jones, D.P., (2011). Living without 30nm chromatin fibers. *Trends Biochem. Sci.*, **36**, 1–6. https://doi.org/10.1016/j.tibs.2010.09.002.
24. Ou, H.D., Phan, S., Deerinck, T.J., Thor, A., Ellisman, M. H., O'Shea, C.C., (2017). ChromEMT: Visualizing 3D chromatin structure and compaction in interphase and mitotic cells. *Science*, **357**, eaag0025. https://doi.org/10.1126/science.aag0025.
25. Li, G., Reinberg, D., (2011). Chromatin higher-order structures and gene regulation. *Curr. Opin. Genet. Dev.*, **21**, 175–186. https://doi.org/10.1016/j.gde.2011.01.022.
26. Ricci, M.A., Manzo, C., García-Parajo, M.F., Lakadamyali, M., Cosma, M.P., (2015). Chromatin fibers are formed by heterogeneous groups of nucleosomes in vivo. *Cell.*, **160**, 1145–1158. https://doi.org/10.1016/j.cell.2015.01.054.
27. Nozaki, T., Imai, R., Tanbo, M., Nagashima, R., Tamura, S., Tani, T., Joti, Y., Tomita, M., Hibino, K., Kanemaki, M. T., Wendt, K.S., Okada, Y., Nagai, T., Maeshima, K., (2017). Dynamic organization of chromatin domains revealed by super-resolution live-cell imaging. *Mol. Cell.*, **67**, 282–293. https://doi.org/10.1016/j.molcel.2017.06.018.
28. Zentgraf, H., Franke, W.W., (1984). Differences of supranucleosomal organization in different kinds of chromatin: cell type-specific globular subunits containing different numbers of nucleosomes. *J. Cell Biol.*, **99**, 272–286. https://doi.org/10.1083/jcb.99.1.272.
29. Ozer, G., Collepardo-Guevara, R., Schlick, T., (2015). Forced unraveling of chromatin fibers with nonuniform linker DNA lengths. *J. Phys. Condens. Matter*, **27**, 64113. https://doi.org/10.1088/0953-8984/27/6/064113.
30. Hsieh, T.-H.S., Weiner, A., Lajoie, B., Dekker, J., Friedman, N., Rando, O.J., (2015). Mapping nucleosome resolution chromosome folding in yeast by Micro-C. *Cell*, **162**, 108–119. https://doi.org/10.1016/j.cell.2015.05.048.
31. Krietenstein, N., Abraham, S., Venev, S.V., Abdennur, N., Gibcus, J., Hsieh, T.-H.S., Parsi, K.M., Yang, L., et al., (2020). Ultrastructural details of mammalian chromosome architecture. *Mol. Cell.*, **78**, 554–565.e7. https://doi.org/10.1016/j.molcel.2020.03.003.
32. Fan, Y., Nikitina, T., Morin-Kensicki, E.M., Zhao, J., Magnuson, T.R., Woodcock, C.L., Skoultchi, A.I., (2003).

H1 linker histones are essential for mouse development and affect nucleosome spacing in vivo. *Mol. Cell. Biol.*, **23**, 4559–4572. https://doi.org/10.1128/MCB.23.13.4559-4572.2003.

33. Verdone, L., Caserta, M., Di Mauro, E., (2005). Role of histone acetylation in the control of gene expression. *Biochem. Cell Biol.*, **83**, 344–353. https://doi.org/10.1139/o05-041.
34. Otterstrom, J., Castells-Garcia, A., Vicario, C., Gomez-Garcia, P.A., Cosma, M.P., Lakadamyali, M., (2019). Super-resolution microscopy reveals how histone tail acetylation affects DNA compaction within nucleosomes in vivo. *Nucleic Acids Res.*, **47**, 8470–8484. https://doi.org/10.1093/nar/gkz593.
35. Collepardo-Guevara, R., Portella, G., Vendruscolo, M., Frenkel, D., Schlick, T., Orozco, M., (2015). Chromatin unfolding by epigenetic modifications explained by dramatic impairment of internucleosome interactions: A multiscale computational study. *J. Am. Chem. Soc.*, **137**, 10205–10215. https://doi.org/10.1021/jacs.5b04086.
36. Zhang, R., Erler, J., Langowski, J., (2017). Histone acetylation regulates chromatin accessibility: Role of H4K16 in inter-nucleosome interaction. *Biophys. J.*, **112**, 450–459. https://doi.org/10.1016/j.bpj.2016.11.015.
37. Lee, J.Y., Orr-Weaver, T.L., (2001). Chromatin. *Encycl. Genet.*,, 340–343. https://doi.org/10.1006/RWGN.2001.0199.
38. G. Bascom, T. Schlick, 5 – Mesoscale Modeling of Chromatin Fibers, in: C. Lavelle, J.-M. Victor (Eds.), Transl. Epigenetics, Academic Press, Boston, 2018, pp. 123–147. 10.1016/B978-0-12-803480-4.00005-3.
39. Arya, G., Schlick, T., (2006). Role of histone tails in chromatin folding revealed by a mesoscopic oligonucleosome model. *Proc. Natl. Acad. Sci.*, **103**, 16236–16241. https://doi.org/10.1073/pnas.0604817103.
40. Sun, J., Zhang, Q., Schlick, T., (2005). Electrostatic mechanism of nucleosomal array folding revealed by computer simulation. *Proc. Natl. Acad. Sci. U. S. A.*, **102**, 8180–8185. https://doi.org/10.1073/pnas.0408867102.
41. Perišić, O., Collepardo-Guevara, R., Schlick, T., (2010). Modeling studies of chromatin fiber structure as a function of DNA linker length. *J. Mol. Biol.*, **403**, 777–802. https://doi.org/10.1016/j.jmb.2010.07.057.
42. Roh, T., Wei, G., Farrell, C.M., Zhao, K., (2007). Genome-wide prediction of conserved and nonconserved enhancers by histone acetylation patterns. *Genome Res.*, **17**, 74–81. https://doi.org/10.1101/gr.5767907.
43. Grigoryev, S.A., Arya, G., Correll, S., Woodcock, C.L., Schlick, T., (2009). Evidence for heteromorphic chromatin fibers from analysis of nucleosome interactions. *Proc. Natl. Acad. Sci.*, **106**, 13317–13322. https://doi.org/10.1073/pnas.0903280106.
44. Jian, H., Vologodskii, A.V., Schlick, T., (1997). A combined wormlike-chain and bead model for dynamic simulations of long linear DNA. *J. Comput. Phys.*, **136**, 168–179. https://doi.org/10.1006/jcph.1997.5765.
45. Lappin, T.R.J., Grier, D.G., Thompson, A., Halliday, H.L., (2006). HOX genes: Seductive science, mysterious mechanisms. *Ulster Med. J.*, **75**, 23–31.
46. P.A. Gomez-Garcia, S. Portillo-Ledesma, M.V. Neguembor, M. Pesaresi, W. Oweis, T. Rohrlich, S. Wieser, E. Meshorer, et al., Mesoscale modeling and single nucleosome tracking reveal remodeling of clutch folding and dynamics in stem cell differentiation, (2020) (Cell Reports, In press).
47. Bascom, G., Myers, C., Schlick, T., (2018). Mesoscale modeling reveals formation of an epigenetically driven hoxc gene hubs. *Proc. Natl. Acad. Sci. USA*, **116**, 4955–4962.
48. Yazdi, P.G., Pedersen, B.A., Taylor, J.F., Khattab, O.S., Chen, Y.Y.-H., Chen, Y.Y.-H., Jacobsen, S.E., Wang, P.H., (2015). Increasing nucleosome occupancy is correlated with an increasing mutation rate so long as DNA repair machinery is intact. *PLoS One*, **10**, e0136574.
49. Cao, K., Lailler, N., Zhang, Y., Kumar, A., Uppal, K., Liu, Z., Lee, E.K., Wu, H., et al., (2013). High-resolution mapping of H1 linker histone variants in embryonic stem cells. *PLOS Genet.*, **9**, e1003417.
50. Mieczkowski, J., Cook, A., Bowman, S.K., Mueller, B., Alver, B.H., Kundu, S., Deaton, A.M., Urban, J.A., et al., (2016). MNase titration reveals differences between nucleosome occupancy and chromatin accessibility. *Nat. Commun.*, **7**, 11485.
51. Arya, G., Zhang, Q., Schlick, T., (2006). Flexible histone tails in a new mesoscopic oligonucleosome model. *Biophys. J.*, **91**, 133–150. https://doi.org/10.1529/biophysj.106.083006.
52. Perišić, O., Portillo-Ledesma, S., Schlick, T., (2019). Sensitive effect of linker histone binding mode and subtype on chromatin condensation. *Nucleic Acid. Res.*, **47**, 4949–4957. https://doi.org/10.1093/nar/gkz234.
53. Luque, A., Collepardo-Guevara, R., Grigoryev, S., Schlick, T., (2014). Dynamic condensation of linker histone C-terminal domain regulates chromatin structure. *Nucleic Acids Res.*, **42**, 7553–7560. https://doi.org/10.1093/nar/gku491.
54. Beard, D.A., Schlick, T., (2001). Computational modeling predicts the structure and dynamics of chromatin fiber. *Structure*, **9**, 105–114. https://doi.org/10.1016/S0969-2126(01)00572-X.
55. Arya, G., Schlick, T., (2009). A tale of tails: How histone tails mediate chromatin compaction in different salt and linker histone environments. *J. Phys. Chem. A*, **113**, 4045–4059. https://doi.org/10.1021/jp810375d.
56. Collepardo-Guevara, R., Schlick, T., (2012). Crucial role of dynamic linker histone binding and divalent ions for DNA accessibility and gene regulation revealed by mesoscale modeling of oligonucleosomes. *Nucleic Acids Res.*, **40**, 8803–8817. https://doi.org/10.1093/nar/gks600.
57. Davey, C.A., Sargent, D.F., Luger, K., Maeder, A.W., Richmond, T.J., (2002). Solvent mediated interactions in the structure of the nucleosome core particle at 1.9 Å resolution. *J. Mol. Biol.*, **319**, 1097–1113. https://doi.org/10.1016/S0022-2836(02)00386-8.
58. Beard, D.A., Schlick, T., (2001). Modeling salt-mediated electrostatics of macromolecules: The discrete surface charge optimization algorithm and its application to the nucleosome. *Biopolymers*, **58**, 106–115. https://doi.org/10.1002/1097-0282(200101)58:1<106::aid-bip100>3.0.co;2-%23.
59. Zhang, Q., Beard, D.A., Schlick, T., (2003). Constructing irregular surfaces to enclose macromolecular complexes for mesoscale modeling using the discrete surface charge optimization (DISCO) algorithm. *J. Comput. Chem.*, **24**, 2063–2074. https://doi.org/10.1002/jcc.10337.
60. Stigter, D., (1977). Interactions of highly charged colloidal cylinders with applications to double-stranded.

Biopolymers, **16**, 1435–1448. https://doi.org/10.1002/bip.1977.360160705.

61. Allan, J., Mitchell, T., Harborne, N., Bohm, L., Crane-Robinson, C., (1986). Roles of H1 domains in determining higher order chromatin structure and H1 location. *J. Mol. Biol.*, **187**, 591–601. https://doi.org/10.1016/0022-2836(86)90337-2.
62. Baumann, C.G., Smith, S.B., Bloomfield, V.A., Bustamante, C., (1997). Ionic effects on the elasticity of single DNA molecules. *Proc. Natl. Acad. Sci. U. S. A.*, **94**, 6185–6190. https://doi.org/10.1073/pnas.94.12.6185.
63. Metropolis, N., Ulam, S., (1949). The Monte Carlo method. *J. Am. Stat. Assoc.*, **44**, 335–341. https://doi.org/10.1080/01621459.1949.10483310.
64. Rosenbluth, M.N., Rosenbluth, A.W., (1955). Monte Carlo calculation of the average extension of molecular chains. *J. Chem. Phys.*, **23**, 356–359. https://doi.org/10.1063/1.1741967.
65. Drew, H.R., Travers, A.A., (1985). DNA bending and its relation to nucleosome positioning. *J. Mol. Biol.*, **186**, 773–790. https://doi.org/10.1016/0022-2836(85)90396-1.
66. Sander, J., Ester, M., Kriegel, H.-P., Xu, X., (1998). Density-based clustering in spatial databases: The algorithm GDBSCAN and its applications. *Data Min. Knowl. Discov.*, **2**, 169–194. https://doi.org/10.1023/A:1009745219419.
67. Ester, M., Kriegel, H.-P., Sander, J., (1996). A density-based algorithm for discovering clusters in large spatial databases with noise. *Proc. 2nd Int. Conf. Knowl. Discov. Data Min.*,, 226–231.
68. Butler, P.J., Thomas, J.O., (1998). Dinucleosomes show compaction by ionic strength, consistent with bending of linker DNA. *J. Mol. Biol.*, **281**, 401–407. https://doi.org/10.1006/jmbi.1998.1954.
69. Garcia-Ramirez, M., Dong, F., Ausio, J., (1992). Role of the histone "tails" in the folding of oligonucleosomes depleted of histone H1. *J. Biol. Chem.*, **267**, 19587–19595.
70. Grigoryev, S.A., Bascom, G., Buckwalter, J.M., Schubert, M.B., Woodcock, C.L., Schlick, T., (2016). Hierarchical looping of zigzag nucleosome chains in metaphase chromosomes. *Proc. Natl. Acad. Sci. USA*, **113**, 1238–1243. https://doi.org/10.1073/pnas.1518280113.
71. Szerlong, H.J., Hansen, J.C., (2011). Nucleosome distribution and linker DNA: Connecting nuclear function to dynamic chromatin structure. *Biochem. Cell Biol.*, **89**, 24–34. https://doi.org/10.1139/O10-139.
72. Bascom, G., Kim, T., Schlick, T., (2017). Kilobase pair chromatin fiber contacts promoted by living-system-like DNA linker length distributions and nucleosome depletion. *J. Phys. Chem. B*, **121**, 3882–3894. https://doi.org/10.1021/acs.jpcb.7b00998.
73. Jiang, C., Pugh, B.F., (2009). Nucleosome positioning and gene regulation: advances through genomics. *Nat. Rev. Genet.*, **10**, 161–172. https://doi.org/10.1038/nrg2522.
74. Happel, N., Doenecke, D., (2009). Histone H1 and its isoforms: contribution to chromatin structure and function. *Gene*, **431**, 1–12. https://doi.org/10.1016/j.gene.2008.11.003.
75. Rao, S.S.P., Huang, S.-C., Glenn St Hilaire, B., Engreitz, J. M., Perez, E.M., Kieffer-Kwon, K.-R., Sanborn, A.L., Johnstone, S.E., et al., (2017). Cohesin loss eliminates all loop domains. *Cell*, **171**, 305–320. https://doi.org/10.1016/j.cell.2017.09.026.
76. Pearson, E.C., Bates, D.L., Prospero, T.D., Thomas, J.O., (1984). Neuronal nuclei and glial nuclei from mammalian cerebral cortex: Nucleosome repeat lengths, DNA contents and H1 contents. *Eur. J. Biochem.*, **144**, 353–360. https://doi.org/10.1111/j.1432-1033.1984.tb08471.x.
77. Anderson, J.D., Widom, J., (2001). Poly(dA-dT) promoter elements increase the equilibrium accessibility of nucleosomal DNA target sites. *Mol. Cell. Biol.*, **21**, 3830–3839. https://doi.org/10.1128/MCB.21.11.3830-3839.2001.
78. Badis, G., Chan, E.T., van Bakel, H., Pena-Castillo, L., Tillo, D., Tsui, K., Carlson, C.D., Gossett, A.J., et al., (2008). A library of yeast transcription factor motifs reveals a widespread function for Rsc3 in targeting nucleosome exclusion at promoters. *Mol. Cell.*, **32**, 878–887. https://doi.org/10.1016/j.molcel.2008.11.020.
79. Hartley, P.D., Madhani, H.D., (2009). Mechanisms that specify promoter nucleosome location and identity. *Cell*, **137**, 445–458. https://doi.org/10.1016/j.cell.2009.02.043.
80. Wiese, O., Marenduzzo, D., Brackley, C.A., (2019). Nucleosome positions alone can be used to predict domains in yeast chromosomes. *Proc. Natl. Acad. Sci. U. S. A.*, **116**, 17307–17315. https://doi.org/10.1073/pnas.1817829116.
81. Efroni, S., Duttagupta, R., Cheng, J., Dehghani, H., Hoeppner, D.J., Dash, C., Bazett-Jones, D.P., Le Grice, S., et al., (2008). Global transcription in pluripotent embryonic stem cells. *Cell Stem Cell*, **2**, 437–447. https://doi.org/10.1016/j.stem.2008.03.021.
82. Routh, A., Sandin, S., Rhodes, D., (2008). Nucleosome repeat length and linker histone stoichiometry determine chromatin fiber structure. *Proc. Natl. Acad. Sci. USA*, **105**, 8872–8877. https://doi.org/10.1073/pnas.0802336105.
83. Robinson, P.J.J., An, W., Routh, A., Martino, F., Chapman, L., Roeder, R.G., Rhodes, D., (2008). 30 nm chromatin fibre decompaction requires both H4–K16 acetylation and linker histone eviction. *J. Mol. Biol.*, **381**, 816–825. https://doi.org/10.1016/j.jmb.2008.04.050.
84. Allfrey, V.G., Faulkner, R., Mirsky, A.E., (1964). Acetylation and methylation of histones and their possible role. *Proc. Natl. Acad. Sci. U. S. A.*, **51**, 786–794. https://doi.org/10.1073/pnas.51.5.786.
85. Meshorer, E., Yellajoshula, D., George, E., Scambler, P.J., Brown, D.T., Misteli, T., (2006). Hyperdynamic plasticity of chromatin proteins in pluripotent embryonic stem cells. *Dev. Cell.*, **10**, 105–116. https://doi.org/10.1016/j.devcel.2005.10.017.
86. Simon, M., North, J.A., Shimko, J.C., Forties, R.A., Ferdinand, M.B., Manohar, M., Zhang, M., et al., (2011). Histone fold modifications control nucleosome unwrapping and disassembly. *Proc. Natl. Acad. Sci. U. S. A.*, **108**, 12711–12716. https://doi.org/10.1073/pnas.1106264108.